ON THE SWAY, YAW AND ROLL MOTIONS OF A SHIP IN SHORT CRESTED WAVES

TASAI, Fukuzo
Research Institute for Applied Mechanics, Kyushu University : Professor

https://doi.org/10.5109/7172170

出版情報：Reports of Research Institute for Applied Mechanics. 19 (62), pp.1-36, 1971. 九州大学応用力学研究所
バージョン：
権利関係：

Reports of Research Institute for Applied Mechanics
Vol. XIX, No. 62, 1971

ON THE SWAY, YAW AND ROLL MOTIONS OF A SHIP IN SHORT CRESTED WAVES

By Fukuzō TASAI*

In this paper, first we have derived two kinds of the equations of the sway, yaw and roll motions in waves based on the strip theory.

One is according to the Ordinary Strip Method and the other according to the New Strip Method.

In the next place, we have measured these three motions for a model ship with full form self-propelling in short crested waves generated in our long towing tank, and compared the results of computation by the above two equations with the results of experiments.

Through the above study, it is concluded that the computed values from the equation of motion by the Ordinary Strip Method differ very little from the ones by the New Strip Method. Comparisons between computed values and experimental ones show satisfactory agreement for the amplitudes of the sway and yaw. As for the amplitudes of the roll in the resonance condition, however, the computed values are larger than the experimental ones by about 10~20 percents.

1. Introduction

The coupled second-order diffential equations based on a strip theory for the heave and pitch motions can predict their amplitudes and phase lags with a considerably good accuracy. Nowadays, these equations are widely used in the investigations on seakeeping qualities for longitudinal motions of a ship.

Concerning the coupled motions of the sway and yaw in oblique waves, we have Eda's method[1] for an approximate computation, whose results show satisfactory agreement with experimental results.

It is, however, hardly investigated as to how effective the equations based on a strip theory are on three coupled motions which include the roll.

In this paper, we have measured these three motions for a model ship self-propelling in short crested waves generated in a long towing tank; on the other hand, we developed two kinds of coupled equations of the sway, yaw and roll motions according to a strip method, and we compared and examined the results of these computations with experimental results.

*Professor, Research Institute for Applied Mechanics, Kyushu University.

2. Short Crested Waves in a Long Towing Tank

In a long towing tank, we can generate regular waves, irregular waves and transient waves[2] by using the wave maker. They are usually, however, long crested waves.

In our long towing tank of Research Institute for Applied Mechanics of Kyushu University, the float of the wave-maker of the plunger type is divided into eight parts. If each of the eight floats is given the amplitude and phase based on computation and made to vertical motion in the same period, we can generate short crested regular waves which are composed of two kinds of one-dimensional waves advancing each other in different directions. Short crested irregular waves can also be generated by varying period of the wave-maker in every cycle.[3]

In Fig. 1, let us introduce the coordinate system O-XYZ fixed in space. The velocity potential ϕ_w of the gravity waves progressing to the X direction can be expressed from the paper (4) as

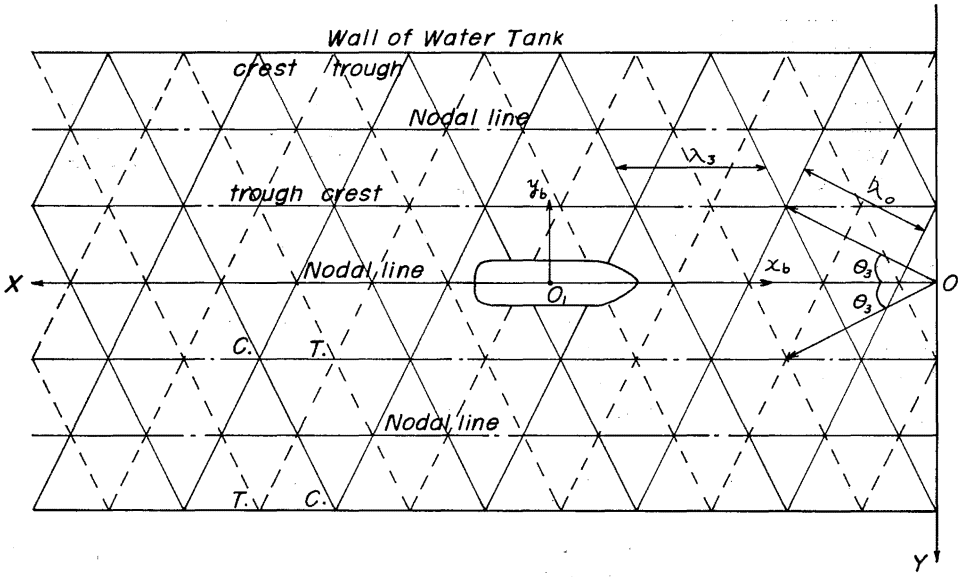

Fig. 1 Three-node wave and coordinate system

$$\phi_w = \frac{\omega \cosh k_0(Z+h)}{k_0 \sinh k_0 h} \sum_{n=0}^{n<B_0k_0/\pi} A_n \cos \frac{n\pi\left(\frac{B_0}{2}+Y\right)}{B_0} \cos\left(\sqrt{k_0^2-\left(\frac{n\pi}{B_0}\right)^2}\, X - \omega t + \varepsilon_n\right)$$

, where B_0 = tank breadth (2.1)

h = water depth

k_0 = wave number of one-dimensional wave

$= \omega^2/g = 2\pi/\lambda_0$

$\lambda_0 =$ wave length of one-dimensional wave

$\omega =$ circular frequency

and $C_0 = \omega/k_0 = \frac{g\lambda_0}{2\pi}\sqrt{\tanh 2\pi h/\lambda_0}$ is the phase velocity of one-dimensional wave.

The elevation ζ of the progressing waves can be written, using the equation (2.1), in the form:

$$\zeta = \sum_{n=0}^{n<B_0k_0/\pi} A_n \cos\frac{n\pi\left(\frac{B_0}{2}+Y\right)}{B_0} \sin\left(\sqrt{k_0{}^2-\left(\frac{n\pi}{B_0}\right)^2}\cdot X-\omega t+\varepsilon_n\right). \tag{2.2}$$

The above equation in the case of $n \neq 0$ shows nodal waves varying amplitude in the Y direction, that is, in the direction of tank breadth. In the case of $n=0$, it does, of course, long crested waves.

The equation (2.2) can also be transformed into the following form:

$$\zeta = \sum_{n=0}^{n<B_0k_0/\pi} \frac{A_n}{2}\left[\sin\left\{k_0\left(\sqrt{1-\left(\frac{n\pi}{B_0k_0}\right)^2}X+\frac{n\pi}{B_0k_0}Y\right)-\omega t+\varepsilon_{n1}\right\}+\right.$$
$$\left.+\sin\left\{k_0\left(\sqrt{1-\left(\frac{n\pi}{B_0k_0}\right)^2}X-\frac{n\pi}{B_0k_0}Y\right)-\omega t+\varepsilon_{n2}\right\}\right] \tag{2.3}$$

, where if n is an even number, ε_{n2} is equal to ε_{n1} and if n is an odd number, ε_{n2} is equal to $\varepsilon_{n1}-\pi$.

Putting $\quad n\pi/B_0k_0 = n\lambda_0/2B_0 = \sin\theta_n \qquad (2.4)$

, we can obtain $\sqrt{1-\left(\frac{n\pi}{B_0k_0}\right)^2} = \cos\theta_n$.

The equation (2.3) presents the waves composed of two kinds of one-dimensional waves, which progress at an angle of $\theta_n = \pm\sin^{-1}(n\pi/B_0k_0)$ to the X axis.

Putting $\lambda_0 = 3$m, $n=2$ and $B_0 = 8$m, we can get $\theta_2 = \sin^{-1}(3/8) \doteqdot 22$ degrees.

Generally, the larger n and λ_0 become, the larger θ_n becomes.

In the next place, we put

$$k_0\cos\theta_n = k_n. \tag{2.5}$$

Let N_0 be the largest integer of $n < B_0k_0/\pi$ and assuming that h of water depth is great enough to be regarded as deep sea waves, (2.1) and (2.2) become

$$\phi_w = \frac{\omega}{k_0}e^{k_0Z}\sum_{n=0}^{N_0} A_n\cos\frac{n\pi}{B_0}\left(\frac{B_0}{2}+Y\right)\cos(k_nX-\omega t+\varepsilon_n) \tag{2.6}$$

$$\zeta = \sum_{n=0}^{N_0} A_n\cos\frac{n\pi}{B_0}\left(\frac{B_0}{2}+Y\right)\sin(k_nX-\omega t+\varepsilon_n). \tag{2.7}$$

N_0 is the maximum number of nodes of all waves in the water tank.

For example, the breadth of our tank is eight meters and therefore, if the maker is given 1.0 sec of period, we obtain 10 of N_0. But the maximum number of node is 5 at $T_w=1.0$ sec, as far as the nodal waves can be generated independently (without superposing of other nodal waves). The details about these points are discussed in the papers (3) and (4).

k_n in the equation (2.5) is the apparent wave number. Letting wave length of nodal wave be λ_n, we get

$$\lambda_n=2\pi/k_n=\lambda_0/\cos\theta_n. \tag{2.8}$$

At the time of $t=0$, supposing that we put at 0 a wave node in the case of n in odd numbers or a wave crest in the case of n in even numbers, ζ_w of the sub-surface and ϕ_w can be written, according to (2.6) and (2.7), in the form:

$$\phi_w=-\frac{\zeta_a\omega}{k_0}e^{k_0Z}\cos\left\{\frac{n\pi}{B_0}\left(\frac{B_0}{2}+Y\right)\right\}\sin(k_nX-\omega t) \tag{2.9}$$

$$\zeta_w=-\zeta_a e^{k_0Z}\cos\left\{\frac{n\pi}{B_0}\left(\frac{B_0}{2}+Y\right)\right\}\cos(k_nX-\omega t) \tag{2.10}$$

, where ζ_a is amplitude of nodal wave and $2\zeta_a=H$ is wave height.

In Fig. 2, 0_1 is the point of intersection of the load water line and the vertical line through G of the center of gravity of a ship when it floats on the still water line. As shown in Figs. 1 and 2, $O_1-x_by_bz_b$ is assumed to be a coordinate system fixed in the ship which puts O_1 at the origin and $G-xyz$ which

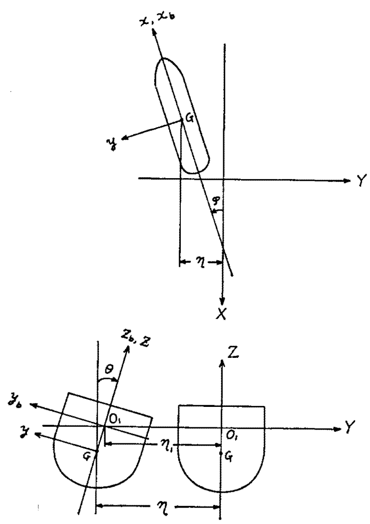

Fig. 2 Coordinate systems

puts G at origin to be a coordinate system fixed in the ship parallel with $O_1-x_b y_b z_b$.

In this paper, we will treat of the case of a ship advancing with constant speed of V in short crested regular waves under the head sea condition.

We assume that OY and $O_1 y_b$ are on the same plane at $t=0$.

When a ship advances without oscillation, that is to say, under the restrained condition, the equation (2.10) can be expressed, using a body axis (x_b, y_b, z_b), as

$$\zeta_w=-\zeta_a e^{k_0 z_b}\cos\left\{\frac{n\pi}{B_0}\left(\frac{B_0}{2}-y_b\right)\right\}\cos(k_n x_b+\omega_e t) \tag{2.11}$$

, where $\omega_e=\omega+k_n V=\omega+k_0 V\cos\theta_n$. (2.12)

The pressure p is given by

$$p=-\rho\frac{\partial\phi_w}{\partial t}=-\rho g\zeta_a e^{k_0 z_b}\cos\left\{\frac{n\pi}{B_0}\left(\frac{B_0}{2}-y_b\right)\right\}\cos(k_n x_b+\omega_e t) \tag{2.13}$$

3. Equations of the Sway, Yaw and Roll Motions in Short Crested Waves

The author has already derived the coupled equations of the sway, yaw and roll motions of a ship with zero speed in beam seas (1965)[5] and ones in oblique waves (1966)[6].

In the latter, we partially considered the effect of the ship speed, but essentially neglected it as for the radiation forces and moments in these equations of motions.

Regarding the pitch and heave motions, the Ordinary Strip Method[7] (hereinafter referred to as the O. S. M.) explains results of experiments rather well, but a more rational strip theory has been developed by Dr. Matao Takagi. Differences between the two are described in Tasai and Takagi[8]*.

Recently, from another approach, N. Salvesen, E. O. Tuck and O. Faltinsen[9] have developed equations of longitudinal motions and lateral motions (hereinafter referred to as the S. T. F. method), where the end effect of the hull is taken into consideration. As for longitudinal motions, Takagi's new equations perfectly accord with the S. T. F. method's excepting the end effect. Furthermore, Salvesen and others[9] have given coupled equations of the sway, yaw and roll motions in oblique waves.

In this chapter, first, we will derive the coupled differential equations of the sway, yaw and roll motions according to the O. S. M. and secondly ones based on Takagi's new strip theory. And they will be compared with those of the S. T. F. method.

In Figs. 1 and 2, it is assumed that a ship advances with constant speed of V oscillating with small amplitudes.

---

* The idea of the new strip theory in the paper (8) is Dr. Takagi's.

Let the angular displacements of the rotational motion about x and z axis be θ and φ respectively, and η be the sway displacement.

Assuming that all ship oscillations are small, we neglect effects of the pitch, heave and surge motions acting upon the sway, yaw and roll motions.

And moreover it is assumed that all viscous effects can be disregarded.

Because we let a model ship self-propel on the center line ($Y=0$) of the water tank for the convenience of experimental equipments, short crested waves with n in odd numbers were used in order to generate the lateral motions.

Table 1 Nomenclature

L :	length between perpendiculars
B :	breadth of ship
d :	draft of ship
m_0 :	mass of ship
W :	weight of displacement of ship
GM :	metacentric height of ship
m :	sectional mass per unit length
w :	sectional weight per unit length
T :	sectional draft
$2b$:	sectional beam of water plane
Sw :	submerged sectional area
GM' :	sectional metacentric height
m' :	sectional added mass for horizontal motion
$m_0\overline{K}_\eta$:	added mass of ship for horizontal motion
N_η :	sectional damping coefficient for horizontal motion
$\overline{N}_\eta$:	damping coefficient of ship for horizontal motion
N_θ :	sectional damping coefficient for rolling motion about x_b axis
l_η :	lever of sectional added inertia moment due to swaying motion
l_w :	lever of sectional damping moment due to swaying motion
l_θ :	lever of sectional added inertia force due to rolling motion about x_b axis
J_x' :	sectional mass moment of inertia about x axis
J_x :	mass moment of inertia of ship about x axis
I'_x :	sectional added mass moment of inertia about x_b axis
I_x :	added mass moment of inertia of ship about x_b axis
I_{xo} :	added mass moment of inertia of ship about x axis
J_z :	mass moment of inertia of ship about z axis
I_z :	added mass moment of inertia of ship about z axis
$F'_{\eta e}$:	sectional exciting force for swaying motion
$F_{\eta e}$:	exciting force of ship for swaying motion
$M'_{e\varphi}$:	sectional exciting moment about z axis
$M_{\varphi e}$:	exciting moment of ship about z axis
$M'_{\theta e}$:	sectional exciting moment about x axis
$M_{\theta e}$:	exciting moment of ship about x axis

And therefore in both theoretical calculations and experiments, we will discuss the sway, yaw and roll motions of a ship advancing in short crested waves with three nodes under the head sea condition.

3.1. Equations of sway, yaw and roll motions based on the O. S. M.

In Fig. 2, let the horizontal displacement of O_1 be η_1, and η_1 is given by

$$\eta_1=\eta-\overline{O_1G}\theta+x_b\varphi. \tag{3.1}$$

Hereafter the nomenclature in Table 1 will be adopted.

In Fig. 1, the momentum of the fluid between the control planes of X and $X+\delta X$ is

$$m'\dot{\eta}_1=m'(\dot{\eta}-\overline{O_1G}\dot{\theta}+x_b\dot{\varphi}-V\varphi). \tag{3.2}$$

According to the O. S. M.[7], therefore, the sway force dF_η/dx_b acting upon an unit length cross section of the hull is written, letting the wave exciting force be $F'_{\eta e}$, in the form:

$$\frac{dF_\eta}{dx_b}=-m(\ddot{\eta}+x_b\ddot{\varphi})-\frac{d}{dt}(m'\dot{\eta}_1)-N_\eta\dot{\eta}_1-\frac{d}{dt}\left(\frac{I'_x\dot{\theta}}{l_\theta}\right)-\frac{N_\theta}{l_w}\dot{\theta}+F'_{\eta e} \tag{3.3}$$

The above equation, being rewritten by using symmetric relations of $I'_x/l_\theta=m'l_\eta$ and $N_\theta/l_w=N_\eta l_w$, becomes

$$\begin{aligned}\frac{dF_\eta}{dx_b}&=-m(\ddot{\eta}+x_b\ddot{\varphi})-m'(\ddot{\eta}-\overline{O_1G}\,\ddot{\theta}+x_b\ddot{\varphi}-2V\dot{\varphi})\\&-N_\eta(\dot{\eta}-\overline{O_1G}\,\dot{\theta}+x_b\dot{\varphi}-V\varphi)-m'l_\eta\ddot{\theta}-N_\eta l_w\dot{\theta}\\&+V(\dot{\eta}-\overline{O_1G}\,\dot{\theta}+x_b\dot{\varphi}-V\varphi)\frac{\partial m'}{\partial x_b}+V\dot{\theta}\frac{\partial}{\partial x_b}(m'l_\eta)+F'_{\eta e}\end{aligned} \tag{3.4}$$

Consequently, equations for the sway and yaw motions are given by

$$\int_L\left(\frac{dF_\eta}{dx_b}\right)dx_b=0,\quad \int_L\left(\frac{dF_\eta}{dx_b}\right)x_b dx_b=0. \tag{3.5}$$

In the next place, the roll moment acting on an unit length cross section about the center of the gravity G is

$$\begin{aligned}\frac{dM_\theta}{dx_b}&=-J'_x\ddot{\theta}-\frac{d}{dt}\left\{(I'_x-\frac{I'_x}{l_\theta}\overline{O_1G})\,\dot{\theta}\right\}-(N_\theta-\frac{N_\theta}{l_w}\overline{O_1G})\dot{\theta}\\&-\frac{d}{dt}\{m'(l_\eta-\overline{O_1G})\dot{\eta}_1\}-N_\eta(l_w-\overline{O_1G})\dot{\eta}_1+F'_{\eta e}(l_w-\overline{O_1G})-w\cdot GM'\,\theta\\&=(-J'_x-I'_x+m'l_\eta\overline{O_1G})\,\ddot{\theta}+V\dot{\theta}\frac{\partial}{\partial x_b}(I'_x-m'l_\eta\overline{O_1G})\\&-N_\eta l_w(l_w-\overline{O_1G})\dot{\theta}-m'\ddot{\eta}_1(l_\eta-\overline{O_1G})+V\dot{\eta}_1\frac{\partial}{\partial x_b}\left\{m'(l_\eta-\overline{O_1G})\right\}\end{aligned}$$

$$-N_\eta(l_w-\overline{O_1G})\dot{\eta}_1-wGM'\theta+F'_{\eta e}(l_w-\overline{O_1G}). \tag{3.6}$$

Then the equation of the roll motion is given by

$$\int_L \left(\frac{dM_\theta}{dx_b}\right)dx_b=0. \tag{3.7}$$

The coupled equations of the sway, yaw and roll motions can be written as follows:

$$\left.\begin{array}{l} a_{11}\ddot{\eta}+a_{12}\dot{\eta}+a_{13}\eta+b_{11}\ddot{\varphi}+b_{12}\dot{\varphi}+b_{13}\varphi+c_{11}\ddot{\theta}+c_{12}\dot{\theta}+c_{13}\theta=F_{\eta e} \\ a_{21}\ddot{\varphi}+a_{22}\dot{\varphi}+a_{23}\varphi+b_{21}\ddot{\theta}+b_{22}\dot{\theta}+b_{23}\theta+c_{21}\ddot{\eta}+c_{22}\dot{\eta}+c_{23}\eta=M_{\varphi e} \\ a_{31}\ddot{\theta}+a_{32}\dot{\theta}+a_{33}\theta+b_{31}\ddot{\eta}+b_{32}\dot{\eta}+b_{33}\eta+c_{31}\ddot{\varphi}+c_{32}\dot{\varphi}+c_{33}\varphi=M_{\theta e} \end{array}\right\} \tag{3.8}$$

Coefficients in (3.8) derived from (3.4), (3.5), (3.6) and (3.7) are shown in Table 2, though; in the calculation of (3.5) and (3.7), we assume that the two-dimensional hydrodynamic force and moment at both ends of the hull are zero, as shown in $[Vm']_{A.P.}^{F.P.}=0$.

Table 2 Coefficients of the Sway, Yaw and Roll Motions

	New Strip Method	O. S. M.
Sway		
$\ddot{\eta}$: a_{11}	$m_0(1+\overline{K}_\eta)$	$m_0(1+\overline{K}_\eta)$
$\dot{\eta}$: a_{12}	$\int_L N_\eta dx_b=\overline{N}_\eta$	$\overline{N}_\eta$
η: a_{13}	0	0
$\ddot{\varphi}$: b_{11}	$\int_L m'x_b dx_b+\frac{V}{\omega_e^2}\int_L N_\eta dx_b$	$\int_L m'x_b dx_b$
$\dot{\varphi}$: b_{12}	$\int_L N_\eta x_b dx_b-V\int_L m'dx_b$	$\int_L N_\eta x_b dx_b-V\int_L m'dx_b$
φ: b_{13}	0	$-V\int_L N_\eta dx_b$
$\ddot{\theta}$: c_{11}	$\int_L m'(l_\eta-\overline{O_1G})dx_b$	$\int_L m'(l_\eta-\overline{O_1G})dx_b$
$\dot{\theta}$: c_{12}	$\int_L N_\eta(l_w-\overline{O_1G})dx_b$	$\int_L N_\eta(l_w-\overline{O_1G})dx_b$
θ: c_{13}	0	0
Yaw		
$\ddot{\varphi}$: a_{21}	$J_z+\int_L m'x_b^2dx_b+\frac{V}{\omega_e^2}\int_L N_\eta x_b dx$	$J_z+\int_L m'x_b^2dx_b$
$\dot{\varphi}$: a_{22}	$\int_L N_\eta x_b^2dx_b+\frac{V^2}{\omega_e^2}\int_L N_\eta dx_b$	$\int_L N_\eta x_b^2dx_b$
φ: a_{23}	$V\int_L N_\eta x_b dx_b-V^2\int_L m'dx_b$	$-V\int_L N_\eta x_b dx_b-V^2\int_L m'dx_b$
$\ddot{\theta}$: b_{21}	$\int_L m'(l_\eta-\overline{O_1G})x_b dx_b$	$\int_L m'(l_\eta-\overline{O_1G})x_b dx_b$

$\dot{\theta}: b_{22}$	$\int_L N_\eta(l_w-\overline{O_1G})x_b \mathrm{d}x_b + V\int_L m'(l_\eta-\overline{O_1G})dx_b$	$\int_L N_\eta(l_w-\overline{O_1G})x_b dx_b + V\int_L m'(l_\eta-\overline{O_1G})dx_b$
$\theta: b_{23}$	$V\int_L N_\eta(l_w-\overline{O_1G})dx_b$	0
$\ddot{\eta}: c_{21}$	$\int_L m'x_b dx_b$	$\int_L m'x_b dx_b$
$\dot{\eta}: c_{22}$	$\int_L N_\eta x_b dx_b + V\int_L m'dx_b$	$\int_L N_\eta x_b dx_b + V\int m'dx_b$
$\eta: c_{23}$	$V\int_L N_\eta dx_b$	0
Roll		
$\ddot{\theta}: a_{31}$	J_x+I_{x0}	J_x+I_{x0}
$\dot{\theta}: a_{32}$	$\int_L N_\eta(l_w-\overline{O_1G})^2 dx_b$	$\int_L N_\eta(l_w-\overline{O_1G})^2 dx_b$
$\theta: a_{33}$	$W\cdot GM$	$W\cdot GM$
$\ddot{\eta}: b_{31}$	$\int_L m'(l_\eta-\overline{O_1G})dx_b$	$\int_L m'(l_\eta-\overline{O_1G})dx_b$
$\dot{\eta}: b_{32}$	$\int_L N_\eta(l_w-\overline{O_1G})dx_b$	$\int_L N_\eta(l_w-\overline{O_1G})dx_b$
$\eta: b_{33}$	0	0
$\ddot{\varphi}: c_{31}$	$\frac{V}{\omega_e^2}\int_L N_\eta(l_w-\overline{O_1G})dx_b + \int_L m'(l_\eta-\overline{O_1G})x_b dx_b$	$\int_L m'(l_\eta-\overline{O_1G})x_b dx_b$
$\dot{\varphi}: C_{32}$	$\int_L N_\eta(l_w-\overline{O_1G})x_b dx_b - V\int_L m'(l_\eta-\overline{O_1G})dx_b$	$\int_L N_\eta(l_w-\overline{O_1G})x_b dx_b - V\int_L m'(l_\eta-\overline{O_1G})dx_b$
$\varphi: c_{33}$	0	$-V\int_L N_\eta(l_w-\overline{O_1G})dx_b$

In the next place, $F'_{\eta e}$ is approximately given, letting the horizontal components of mean orbital velocity and mean orbital acceleration of water particle be $\bar{v}_\eta$ and $\dot{\bar{v}}_\eta$, in the form:

$$F'_{\eta e} \doteqdot F'_{\eta 1} + \frac{d}{dt}(m'\bar{v}_\eta) + N_\eta \bar{v}_\eta = F'_{\eta 1} + m'\dot{\bar{v}}_\eta + N_\eta \bar{v}_\eta - V\bar{v}_\eta \frac{\partial m'}{\partial x_b} \tag{3.9}$$

, where $F'_{\eta 1}$ is Froude-Kriloff's force.

Now, under the condition in head waves with three nodes, ϕ_w becomes

$$\phi_w = \frac{\zeta_a \omega}{k_0} e^{k_0 Z} \cos\left\{\frac{3\pi}{B_0}\left(\frac{B_0}{2} + Y\right)\right\} \sin(k_3 x_b + \omega_e t). \tag{3.10}$$

And therefore, v_η of orbital velocity of water particle in the $-Y$ direction is

$$v_\eta = -\left(\frac{\partial \phi_w}{\partial Y}\right) = -\zeta_a \omega e^{k_0 Z} \sin\theta_3 \cos\left(\frac{3\pi}{B_0} Y\right) \sin(k_3 x_b + \omega_e t) \tag{3.11}$$

Assuming that $\bar{v}_\eta$ and $\dot{\bar{v}}_\eta$ are approximately expressed as the value at $Z=-T/2$ on the center plane of the ship, we obtain the following:

$$\left.\begin{aligned} \bar{v}_\eta &\doteqdot -\zeta_a \omega e^{-k_0 T/2} \sin\theta_3 \sin(k_3 x_b + \omega_e t) \\ \dot{\bar{v}}_\eta &\doteqdot -\zeta_a \omega^2 e^{-k_0 T/2} \sin\theta_3 \cos(k_3 x_b + \omega_e t) \end{aligned}\right\} \tag{3.12}$$

From (3.9) and (3.12), we can calcuate the whole sway exciting force $F_{\eta e} = \int_L F'_{\eta e}\, dx_b$ and the yaw exciting moment $M_{\varphi e} = \int_L F'_{\eta e} x_b dx_b$.

Putting here

$$\left.\begin{aligned} F_{\eta e}/\zeta_a &= \bar{F}_{\eta c} \cos\omega_e t + \bar{F}_{\eta s} \sin\omega_e t \\ M_{\varphi e}/\zeta_a &= \bar{M}_{\varphi c} \cos\omega_e t + \bar{M}_{\varphi s} \sin\omega_e t \end{aligned}\right\} \tag{3.13}$$

, we can obtain

$$\left.\begin{aligned} \bar{F}_{\eta c} = &-\rho g \int_L k_0 S_w S_0 \cos k_3 x_b dx_b \\ &- \omega\omega_e \sin\theta_3 \int_L m' e^{-k_0 T/2} \cos k_3 x_b dx_b \\ &- \omega \sin\theta_3 \int_L N_\eta e^{-k_0 T/2} \sin k_3 x_b dx_b \\ \bar{F}_{\eta s} = &-\rho g \int_L k_0 S_w S_0 \sin k_3 x_b dx_b \\ &+ \omega\omega_e \sin\theta_3 \int_L m' e^{-k_0 T/2} \sin k_3 x_b dx_b \\ &- \omega \sin\theta_3 \int_L N_\eta e^{-k_0 T/2} \cos k_3 x_b dx_b \end{aligned}\right\} \tag{3.14}$$

, where $S_0 = \dfrac{-2}{k_0 S_w} \displaystyle\int_0^{-T} e^{k_0 z_b} \sin(c_3 y_b) dz_b$ (3.15)

and $c_3 = 3\pi/B_0$ ($B_0 = 8\,m$ in our long towing tank).

$$\left.\begin{aligned} \bar{M}_{\varphi c} = &-\rho g \int_L k_0 S_w S_0 x_b \cos k_3 x_b dx_b \\ &- \omega\omega_e \sin\theta_3 \int_L m' e^{-k_0 T/2} x_b \cos k_3 x_b dx_b \\ &- \omega V \sin\theta_3 \int_L m' e^{-k_0 T/2} \sin k_3 x_b dx_b \\ &- \omega \sin\theta_3 \int_L N_\eta e^{-k_0 T/2} x_b \sin k_3 x_b dx_b, \\ \bar{M}_{\varphi s} = &\ \rho g \int_L k_0 S_w S_0 x_b \sin k_3 x_b dx_b \end{aligned}\right\} \tag{3.16}$$

$$
\left.\begin{aligned}
&+\omega\omega_e \sin\theta_3 \int_L m' e^{-k_0 T/2} x_b \sin k_3 x_b dx_b \\
&-\omega V \sin\theta_3 \int_L m' e^{-k_0 T/2} \cos k_3 x_b dx_b \\
&-\omega \sin\theta_3 \int_L N_\eta e^{-k_0 T/2} x_b \cos k_3 x_b dx_b
\end{aligned}\right\}
$$

In the next place, putting the roll exciting moment as follows:

$$M_{\theta e}=M_{\theta 1}+M_{\theta 2}+M_{\theta 3}+M_{\theta 4} \tag{3.17}$$

, we can approximately obtain such as: [10]

$M_{\theta 1}$=moment based on Froude-Kriloff's theory

$$M_{\theta 2}=\int_L m' \bar{v}_\eta (l_\eta - \overline{O_1 G}) dx_b$$

$$M_{\theta 3}=\int_L N_\eta \bar{v}_\eta (l_w - \overline{O_1 G}) dx_b$$

$$
\begin{aligned}
M_{\theta 4}&=-V\int_L \bar{v}_\eta \frac{\partial}{\partial x_b}\left\{m'(l_\eta - \overline{O_1 G})\right\} dx_b \\
&=V\int_L \left\{\overline{O_1 G}\frac{\partial m'}{\partial x_b} - \frac{\partial}{\partial x_b}(m' l_\eta)\right\} \bar{v}_\eta dx_b.
\end{aligned}
$$

Consequently, putting

$$M_{\theta e}/\zeta_a=\overline{M}_{\theta c}\cos\omega_e t+\overline{M}_{\theta s}\sin\omega_e t \tag{3.18}$$

$\overline{M}_{\theta c}$ and $\overline{M}_{\theta s}$ are given by

$$
\left.\begin{aligned}
\overline{M}_{\theta c}=&\rho g \int_L k_0 S_w \left\{S_0 \overline{O_1 G}+(P_0-R_0)T\right\} \cos k_3 x_b dx_b \\
&-\omega\omega_e \sin\theta_3 \int_L m'(l_\eta - \overline{O_1 G}) e^{-k_0 T/2} \cos k_3 x_b dx_b \\
&-\omega \sin\theta_3 \int_L N_\eta (l_w - \overline{O_1 G}) e^{-k_0 T/2} \sin k_3 x_b dx_b \\
\overline{M}_{\theta s}=&-\rho g \int_L k_0 S_w \left\{S_0 \overline{O_1 G}+(P_0-R_0)T\right\} \sin k_3 x_b dx_b \\
&+\omega\omega_e \sin\theta_3 \int_L m'(l_\eta - \overline{O_1 G}) e^{-k_0 T/2} \sin k_3 x_b dx_b \\
&-\omega \sin\theta_3 \int_L N_\eta (l_w - \overline{O_1 G}) e^{-k_0 T/2} \cos k_3 x_b dx_b
\end{aligned}\right\} \tag{3.19}
$$

where

$$P_0-R_0=\frac{2}{k_0\,T\,S_w}\left(\int_0^b e^{k_0 z_b}y_b\sin c_3y_b dy_b-\int_0^{-T} e^{k_0 z_b}z_b\sin c_3y_b dz_b\right) \qquad (3.20)$$

3. 2. Equations of the sway, yaw and roll motions based on Takagi's new strip theory

Dr. Takagi[8] has developed the equations of longitudinal motions which seem to be more rational than those of the O. S. M.. We will derive the equations of lateral motions from Takagi's new strip theory.

In Fig. 2, a certain point (X, Y) on the space-fixed coordinate system can be expressed by (x_b, y_b) of the hull fixed coordinates as the following form:

$$-y_b=(Y+\eta)-\overline{O_1G}\,\theta+(X-Vt)\varphi,$$
$$x_b=X-Vt.$$

Putting U for the fluid velocity in the $-Y$ direction on the fixed cross section of the hull, U is

$$U=-(\dot{\eta}-\overline{O_1G}\,\dot{\theta}+x_b\dot{\varphi}-V\varphi). \qquad (3.21)$$

Under the assumption that $-(\phi_S+i\phi_A)$ is the two dimensional velocity potential when an arbitrary cross section oscillates with periodic velocity $e^{i\omega_e t}$, ϕ_{r1} of two dimensional radiation potential is given by

$$\phi_{r1}=U\ (\phi_S+i\phi_A). \qquad (3.22)$$

For the sway, yaw and roll motions, putting as follows:

$$\left.\begin{aligned}\eta&=\eta_a e^{i(\omega_e t+\varepsilon_\eta)}\\ \varphi&=\varphi_a e^{i(\omega_e t+\varepsilon_\varphi)}\\ \theta&=\theta_a e^{i(\omega_e t+\varepsilon_\theta)}\end{aligned}\right\} \qquad (3.23)$$

, ϕ_{r1} becomes

$$\phi_{r1}=\omega_e\phi_A\eta-\phi_S\dot{\eta}+(V\phi_S+\omega_e x_b\phi_A)\varphi$$
$$+\left(\frac{V}{\omega_e}\phi_A-x_b\phi_S\right)\dot{\varphi}-\omega_e\overline{O_1G}\,\phi_A\theta+\overline{O_1G}\,\phi_S\dot{\theta}. \qquad (3.24)$$

Now, let the whole velocity potential be Φ, and we can calculate the pressure by the following linear equation derived from the Bernoulli equation

$$p-p_a=-\rho g z_b-\rho\left(\frac{\partial}{\partial t}-V\frac{\partial}{\partial x_b}\right)\Phi \qquad (3.25)$$

, where

$$\Phi=\phi_w+\phi_r+\phi_d \qquad (3.26)$$

$\phi_w=$ incident wave potential

$\phi_r=$ radiation wave potential

$\phi_d=$ diffraction wave potential.

Fisrt of all we compute the pressure $p_1^{(r)}$ from ϕ_{r1} and obtain the following:

$$
\begin{aligned}
p_1^{(r)}=\rho\Big[&\phi_s\ddot{\eta}-\left(\omega_e\phi_A+V\frac{\partial\phi_s}{\partial x_b}\right)\dot{\eta}+V\omega_e\frac{\partial\phi_A}{\partial x_b}\eta-\left(\frac{V}{\omega_e}\phi_A-x_b\phi_s\right)\ddot{\varphi}\\
&-\left(2V\phi_s+\omega_e x_b\phi_A-\frac{V^2}{\omega_e^2}\frac{\partial\phi_A}{\partial x_b}+Vx_b\frac{\partial\phi_s}{\partial x_b}\right)\dot{\varphi}+\left(V^2\frac{\partial\phi_s}{\partial x_b}+V\omega_e x_b\frac{\partial\phi_A}{\partial x_b}\right.\\
&\left.+V\omega_e\phi_A\right)\varphi-\overline{O_1G}\phi_s\ddot{\theta}+\left(\omega_e\overline{O_1G}\,\phi_A+V\overline{O_1G}\frac{\partial\phi_s}{\partial x_b}\right)\dot{\theta}\\
&-V\omega_e\overline{O_1G}\frac{\partial\phi_A}{\partial x_b}\theta\Big].
\end{aligned}
\tag{3.27}
$$

In the next place, putting the following for the radiation potential when the ship rolls about x_b axis

$$\phi_{r2}=-(\phi'_S+i\phi'_A)\,\dot{\theta}=-\phi'_S\dot{\theta}+\phi'_A\omega_e\theta \tag{3.28}$$

and substituting this into (3.25), pressure $p_2^{(r)}$ becomes

$$p_2^{(r)}=\rho\left[\phi'_S\ddot{\theta}-\phi'_A\omega_e\dot{\theta}-V\frac{\partial\phi'_S}{\partial x_b}\dot{\theta}+V\frac{\partial\phi'_A}{\partial x_b}\omega_e\theta\right]. \tag{3.29}$$

Therefore, the whole radiation pressure $p^{(r)}$ is given by

$$p^{(r)}=p_1^{(r)}+p_2^{(r)}. \tag{3.30}$$

Herein, taking into consideration the following:

$$
\left.
\begin{aligned}
&2\rho\int_{-T}^{0}\phi_s dz_b=-m', && 2\rho\int_{-T}^{0}\phi_A dz_b=\frac{N_\eta}{\omega_e},\\
&2\rho\int_{-T}^{0}\left(\frac{\partial\phi_s}{\partial x_b}\right)dz_b=-\frac{\partial m'}{\partial x_b}, && 2\rho\int_{-T}^{0}\left(\frac{\partial\phi_A}{\partial x_b}\right)dz_b=\frac{1}{\omega_e}\frac{\partial N_\eta}{\partial x_b},\\
&2\rho\int_{-T}^{0}\phi'_s dz_b=-m'l_\eta, && 2\rho\int_{-T}^{0}\phi'_A dz_b=\frac{1}{\omega_e}N_\eta l_w,\\
&2\rho\int_{-T}^{0}\left(\frac{\partial\phi'_s}{\partial x_b}\right)dz_b=-\frac{\partial}{\partial x_b}(m'l_\eta), && 2\rho\int_{-T}^{0}\left(\frac{\partial\phi'_A}{\partial x_b}\right)dz_b=\frac{1}{\omega_e}\frac{\partial(N_\eta l_w)}{\partial x_b},
\end{aligned}
\right\}
\tag{3.31}
$$

and making use of (3.27), (3.29) and (3.30), we can calculate the force $dF_{\eta 0}/dx_b$ in the $-Y$ direction acting upon an unit length cross section as shown in the following form:

$$
\begin{aligned}
-\frac{dF_{\eta 0}}{dx_b}=&\,m'\ddot{\eta}+\left(N_\eta-V\frac{\partial m'}{\partial x_b}\right)\dot{\eta}-V\frac{\partial N_\eta}{\partial x_b}\eta+\left(m'x_b+\frac{V}{\omega_e^2}N_\eta\right)\ddot{\varphi}\\
&+\left(N_\eta x_b-\frac{V^2}{\omega_e^2}\frac{\partial N_\eta}{\partial x_b}-2Vm'-Vx_b\frac{\partial m'}{\partial x_b}\right)\dot{\varphi}+\left(V^2\frac{\partial m'}{\partial x_b}-VN_\eta-\right.
\end{aligned}
$$

$$- Vx_b\frac{\partial N_\eta}{\partial x_b}\Big)\varphi+m'(l_\eta-\overline{O_1G})\ddot{\theta}+\Big\{(l_w-\overline{O_1G})N_\eta+V\overline{O_1G}\frac{\partial m'}{\partial x_b}-$$

$$-V\frac{\partial}{\partial x_b}(m'l_\eta)\Big\}\dot{\theta}-V\Big\{\frac{\partial(N_\eta l_w)}{\partial x_b}-\overline{O_1G}\frac{\partial N_\eta}{\partial x_b}\Big\}\theta. \tag{3.32}$$

Coefficients for the sway and yaw motions in the left side of the equation (3.8) are computed from

$$\int_L \Big(m\ddot{\eta}-\frac{dF_{\eta 0}}{dx_b}\Big)dx_b \text{ and } \int_L \Big(m\ddot{\eta}-\frac{dF_{\eta 0}}{dx_b}\Big)x_b dx_b.$$

These coefficients are also shown in Table 2.

The roll moment M_{0r} caused by $p^{(r)}$ is written, using the pressure difference $p_0{}^{(r)}=p^{(r)}_{yb}-p^{(r)}_{-yb}$ at the symmetric points on the cross section contour, as

$$M_{0r}=\int_0^b p_0{}^{(r)}y_b dy_b+\int_{-T}^{-\overline{O_1G}} p_0{}^{(r)}z_b dz_b. \tag{3.33}$$

Hereafter let us use the shortened signs of

$$\rho[\phi_s] \text{ for } \rho\Big[\int_0^b \phi_s y_b dy_b+\int_{-T}^{-\overline{O_1G}}\phi_s z_b dz_b\Big].$$

Using these signs, we obtain the following:

$$\left.\begin{aligned}
&\rho[\phi_s]=-m'(l_\eta-\overline{O_1G}), && \rho[\phi_A]=\frac{N_\eta}{\omega_e}(l_w-\overline{O_1G}),\\
&\rho\Big[\frac{\partial\phi_s}{\partial x_b}\Big]=-\frac{\partial}{\partial x_b}\{m'(l_\eta-\overline{O_1G})\}, && \rho\Big[\frac{\partial\phi_A}{\partial x_b}\Big]=\frac{1}{\omega_e}\frac{\partial}{\partial x_b}\{N_\eta(l_w-\overline{O_1G})\},\\
&\rho[\phi'_s]=-(I'_x-m'l_\eta\overline{O_1G}), && \rho[\phi'_A]=\frac{-1}{\omega_e}N_\eta(l_w-\overline{O_1G})l_w,\\
&\rho\Big[\frac{\partial\phi'_s}{\partial x_b}\Big]=-\frac{\partial}{\partial x_b}(I'_x-m'l_\eta\overline{O_1G}), && \rho\Big[\frac{\partial\phi'_A}{\partial x_b}\Big]=\frac{-1}{\omega_e}\frac{\partial}{\partial x_b}\{N_\eta(l_w-\overline{O_1G})\,l_w\}.
\end{aligned}\right\} \tag{3.34}$$

Taking the above into consideration, we will calculate the roll moment acting upon an unit length cross section.

That is as follows:

$$-\frac{dM_{0r}}{dx_b}=(I_x'-2m'l_\eta\overline{O_1G}+m'l_\eta\overline{O_1G^2})\ddot{\theta}$$

$$+\Big[N_\eta(l_w-\overline{O_1G})^2+V\frac{\partial}{\partial x_b}(I'_x-m'l_\eta\overline{O_1G})+V\overline{O_1G}\frac{\partial}{\partial x_b}\{m'(l_\eta-\overline{O_1G})\}\Big]\dot{\theta}$$

$$-\Big[V\frac{\partial}{\partial x_b}\{N_\eta l_w(l_w-\overline{O_1G})\}+V\overline{O_1G}\frac{\partial}{\partial x_b}\{N_\eta(l_w-\overline{O_1G})\}\Big]\theta+$$

$$+\Big[\frac{V}{\omega_e^2}N_\eta(l_w-\overline{O_1G})+x_b\{m'(l_\eta-\overline{O_1G})\}\Big]\ddot{\varphi}$$

$$+\left[N_\eta(l_w-\overline{O_1G})x_b-\frac{V^2}{\omega_e^2}\frac{\partial}{\partial x_b}\{N_\eta(l_w-\overline{O_1G})\}+Vx_b\frac{\partial}{\partial x_b}\{m'(l_\eta-\overline{O_1G})\}\right]\dot{\varphi}$$

$$+\left[V^2\frac{\partial}{\partial x_b}\{m'(l_\eta-\overline{O_1G})\}-VN_\eta(l_w-\overline{O_1G})-Vx_b\frac{\partial}{\partial x_b}\{N_\eta(l_w-\overline{O_1G})\}\right]\varphi$$

$$+m'(l_\eta-\overline{O_1G})\ddot{\eta}+\left[N_\eta(l_w-\overline{O_1G})-V\frac{\partial}{\partial x_b}\{m'(l_\eta-\overline{O_1G})\}\right]\dot{\eta}$$

$$-V\frac{\partial}{\partial x_b}\{N_\eta(l_w-\overline{O_1G})\}\ \eta. \tag{3.35}$$

Coefficients of a_{31}, a_{32}, ... c_{33} are also shown in Table 2. a_{33}, that is, coefficient of restoring moment of the roll is assumed to be $W\cdot GM$.

The above radiation forces were calculated by assuming that the fluid is perfect fluid. In the roll motion, however, viscous resistance is pretty large because of the eddy-making resistance caused by bilge keel and the skin friction of the hull. And consequently a_{32} should include viscous damping coefficient in order to correctly predict the roll motion. This will be discussed in chapter 5.

3.3. Differences in the coefficients of equations of motions

We will compare the coefficients of equations based on the O. S. M., Takagi's new strip method and the S. T. F. method with each other.

The end effect of the hull is considered in the S. T. F. method. Excepting this end effect, however, the coefficients of the S. T. F. method and those by Takagi's new strip method show agreement. For example, coefficients of $\ddot{\varphi}$ and φ can be written as in Table 3. Because φ is a periodic function of ω_e, we obtain $a_{23}\varphi=-\frac{a_{23}}{\omega_e^2}\ddot{\varphi}$. Including a_{23} in a_{21}, we get

$$a_{21}=J_z+\int_L m'x_b^2dx_b+\frac{V}{\omega_e^2}\int_L N_\eta x_b dx_b-\frac{V}{\omega_e^2}\int N_\eta x_b dx_b+\frac{V^2}{\omega_e^2}\int_L m'dx_b.$$

Table 3 Comparison of coefficients

	S. T. F. Method	New Strip Method
$\ddot{\varphi}$: a_{21}	$J_z+\int_L m'x_b^2dx_b+\frac{V^2}{\omega_e^2}\int_L m'dx_b$	$J_z+\int_L m'x_b^2dx_b+\frac{V}{\omega_e^2}\int_L N_\eta x_b dx_b$
φ : a_{23}	0	$V\int_L N_\eta x_b dx_b-V^2\int_L m'dx_b$

And therefore, this accords with the one by the S. T. F. method.

In the next place, differences in the coefficients between the new strip theory and the O. S. M. essentially admitted only for the yaw motion. This says that there are no differences in coefficients for the sway and roll between both methods.

Differences exist for a_{22}, a_{23}, b_{23} **and** c_{23} of the yaw. As shown on page 31 in the paper (8), differences in coefficients for the longitudinal motions between Takagi's new strip method and the O. S. M. don't appear in the equation for the heave but in the one for the pitch. This resembles the case of the above lateral motions.

3.4. Diffraction wave force

We will derive the diffraction wave force using Takagi's new strip method.

It is assumed that the equation (3.12) can approximately show the component in the $-$Y direction of the orbital velocity of water particles. The equation is

$$\bar{v}_\eta \doteqdot -\zeta_a \omega e^{-k_0 T/2} \sin\theta_3 \sin(k_3 x_b + \omega_e t).$$

Using $\bar{v}_\eta$, the diffraction wave potential ϕ_d can be approximately given by

$$\phi_d = \bar{v}_\eta(\phi_s + i\phi_A). \tag{3.36}$$

From (3.36) and (3.25), we can obtain

$$p^{(d)} = -\rho\dot{\bar{v}}_\eta\phi_s + \rho\omega\bar{v}_\eta\phi_A + \rho V\left(\bar{v}_\eta\frac{\partial\phi_s}{\partial x_b} - \omega\eta_w\frac{\partial\phi_A}{\partial x_b}\right)$$

, where

$$\left.\begin{aligned} \dot{\bar{v}}_\eta &= -\zeta_a\omega^2 e^{-k_0 T/2}\sin\theta_3\cos(k_3 x_b + \omega_e t) \\ \eta_w &= \zeta_a e^{-k_0 T/2}\sin\theta_3\cos(k_3 x_b + \omega_e t). \end{aligned}\right\} \tag{3.37}$$

Using (3.31) and computing the sway exciting force and yaw moment, we find that the sway force agrees with the one by the O. S. M., though; as for the yaw moment, the following terms are added to the one by the O. S. M.

$$\left.\begin{aligned} M_{\varphi c}/\zeta_a &= \frac{V\omega}{\omega_e}\cdot\sin\theta_3\int_L e^{-k_0 T/2} N_\eta \cos k_3 x_b dx_b \\ M_{\varphi s}/\zeta_a &= -\frac{V\omega}{\omega_e}\sin\theta_3\int_L e^{-k_0 T/2} N_\eta \sin k_3 x_b dx_b \end{aligned}\right\}. \tag{3.38}$$

The roll exciting moment $M_{\theta e}$ computed by using (3.30) and (3.34) accords with the equation (3.19) obtained by the O. S. M..

As can be seen above, differences in the diffraction wave force between Takagi's new strip method and the O. S. M. exist only for $M_{\varphi e}$. Concerning the sway exciting force and roll moment, both methods show perfect agreement.

The equations of the yaw moment added to those of the O. S. M. resemble the terms of $\sim\!\sim\!\sim$ on page 31 in the paper (8).

4. Model Experiments

We used the N-ship model which was described in the paper "A Study on

Seakeeping Qualities of Full Ships".[11] The principal particulars of the model are shown in Table 4 and the body plan in Fig. 3.

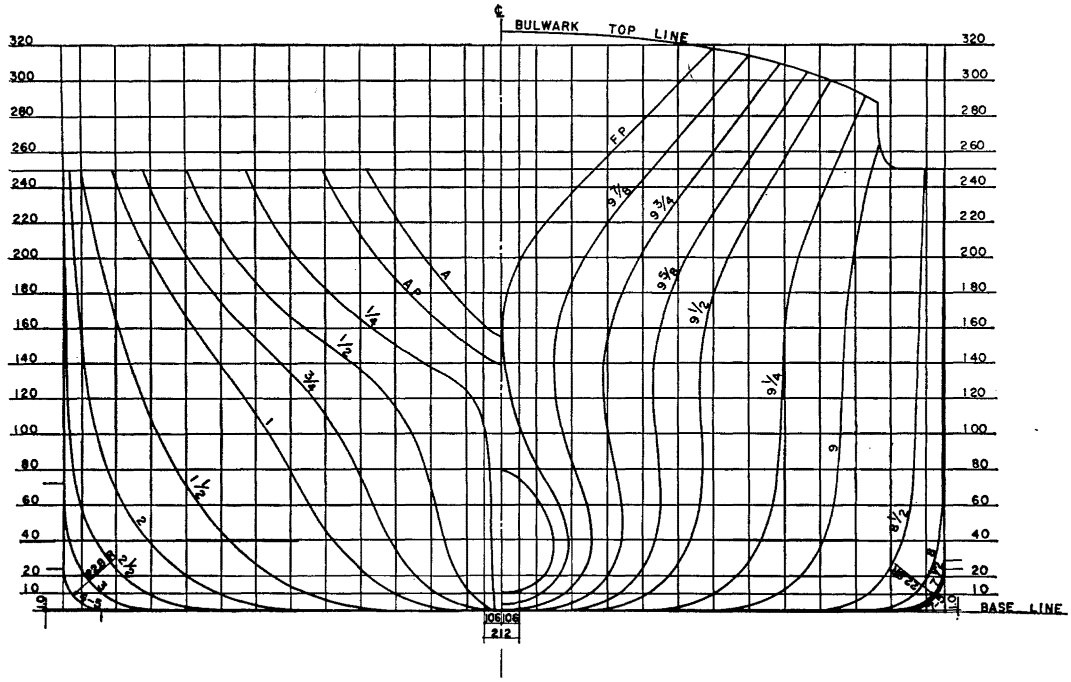

Fig. 3 Bodyplan of the model ship

Table 4 Principal particulars of the model ship

Description		Model Ship
Length between perpendiculars	L	3.00 m
Breadth	B	0.5012 m
Depth	D	0.2500 m
Draft	d	0.1686 m
Displacement	W	206.48 kg
Block coefficient	C_B	0.815
Waterplane area coefficient	C_w	0.870
Prismatic coefficient	C_p	0.822
Center of buoyancy forward of midship		0.0655 m
Center of waterplane area forward of midship		-0.001 m
Radius of gyration for pitch and yaw		0.235 L
GM		0.072 m
$\overline{O_1G}$		0.0336 m
Natural rolling period	T_θ	1.244 sec

Without bilge keel. With rudder and propeller.

The experiments under the full load condition were carried out in the large tank ($L \times B \times D \times d = 80m \times 8m \times 3.5m \times 3m$) at the Research Institute for Applied Mechanics of Kyushu University.

4.1. Free rolling experiments of the advancing ship model

We made free rolling experiments of the model advancing in the still water.

The experimental equipment are shown in Fig. 4. The sway displacement is perfectly restrained by the two guiding devices (the rolling axis is pivoted).

Towing Apporatus and Guide Devices

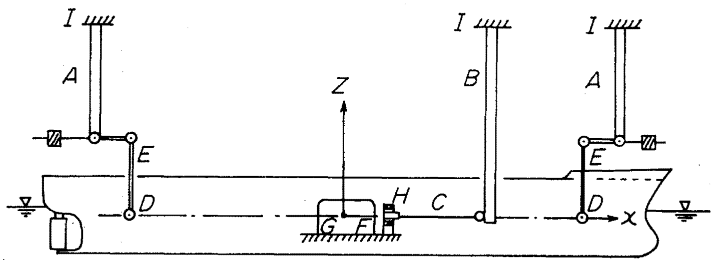

A : Rolling guide
B : Towing rod
C : Piano wire
D : Pivot part
E : Trimmer
F : Vertical gyro
G : Center of Gravity of the model
H : Ball bearing
I : Truck

Fig. 4 Towing apparatus and guide devices

The ship model was towed by the piano wire joined to the towing rod. A ball bearing was used where the piano wire was joined to the hull in order to lessen the effect of the twisting moment of the piano wire. The effect of the friction of each part is small enough to neglect.

The angular displacement of the roll was measured by the vertical gyroscope.

Experiments were conducted by varying the initial heeling angle θ_i as follows: 5°, 10°, 15°, 18°. The extinction curve in the experiment of $\theta_i = 18°$ is assumed to be $\Delta\theta = a\theta_m + b\theta_m^2$. In Fig. 5 are shown a and b (1/deg) of coefficients satisfying both $\theta_m = 5°$ and $\theta_m = 10°$ of the mean rolling angle.

Within the Froude number Fn used in experiments, a increased and b slightly decreased with the increase of the ship speed.

Furthermore, we calculated the mean value of Bertin's extinction coefficient $N = \Delta\theta/\theta_m^2$ for $\theta_m = 8°$, 10° and 12°. It slightly decreased with the increase of ship speed, as shown in Table 5.

Table 5 Experimental values of N coefficient

F_n	0	0.10	0.13	0.16	0.20
N	0.0092	0.0089	0.0088	0.0087	0.0085

On the other hand, the value of N in the case of $\theta_m=10^\circ$ at zero speed which was obtained from Watanabe and others[12] was 0.0064.

4.2. Experiments in head waves with three nodes

We let the model ship self-propel on the node line in three nodal waves and measured the amplitude of the sway, yaw, roll motions and the relative bow motion.

We carried out experiments under the head sea condition, so that we might get the roll resonance for each speed of our ship model with a short natural rolling period. (In the case of a container ship model whose natural rolling period is relatively long would be adopted the following waves.)

Motions of the ship model were measured by means of the equipment for measuring six motions of a ship model[13]. Moreover, in order to measure the amplitudes of the roll and yaw were used angular differential transformers.

We used a manual steering apparatus in order not to let the model get off the nodal line in three nodal waves and the model ship was steered as few times as possible to lessen the effect of steering on the roll motion.

The test conditions in waves were as follows:

$$\lambda_0/L=0.5\sim1.7,$$
$$H/\lambda_0\doteqdot1/50.$$

The wave height H was measured on the crest and trough line at the distance of $B_0/6$ from the center line of the tank.

Some illustrations of records of ship motions are shown in Figs. 6 and 7.

In the analysis of the experimental results, we used the records while the model wasn't steered, as shown in Figs. 6 and 7.

5. Comparison between Experiments and Computations

5.1. Computations of ship motions

Computations of the sway, yaw and roll motions were carried out according to the O. S. M. and the new strip method, by using coefficients of a_{11}, a_{12}, ..., c_{33} in Table 2 and the wave exciting force in (3.13)$\sim$(3.20) and (3.38).

The two dimensional values of m′, l_η, l_w and N_η were calculated by approximating the cross section of the hull to the Lewis form.

For the following items, we used experimental results.

1) Apparent moment of inertia for the roll

Because there's little knowledge about the three dimensional effect for I_x, in this paper we calculated J_x+I_x from the following equation, using the natural rolling period T_θ obtained from the free rolling experiment in the case of $V=0$.

$$T_\theta \doteqdot 2\pi\sqrt{(J_x+I_x)/W\cdot GM}. \tag{5.1}$$

2) Damping coefficient a_{32} for the roll

In order to consider the viscous roll damping moments in addition to the wave damping, we used, in this paper, the damping coefficient obtained from the free rolling experiments. (In principle, it is more rational to get it from the experiments by the forced oscillation method.)

As shown in Watanabe[14] and Tasai[5], equivalent linear roll damping is

$$a_{32}/J_x+I_x=2\alpha_e=\frac{2}{\pi}\omega_\theta\ (a+b\Lambda\theta_a) \tag{5.2}$$

, where $\omega_\theta=2\pi/T_\theta$, $\Lambda=T_\theta/T_e=\omega_e/\omega_\theta$ and T_e is period of encounter.

Putting

$$\Theta_w=\pi H/\lambda_0, \tag{5.3}$$

$$\theta_a=\Theta_w\ \overline{\theta} \tag{5.4}$$

, the equation (5.2) can be written in the form

$$a_{32}=(J_x+I_x)\frac{4}{T_\theta}\left\{a+b\frac{T_\theta}{2\pi}(\omega+k_3V)\Theta_w\ \overline{\theta}\right\}. \tag{5.5}$$

Using $H/\lambda_0\doteqdot 1/50$ in the case of experiments, that is, $\Theta_w=3.6°$; the equation (5.5) becomes as

$$a_{32}=g_1a+g_2b(\omega+k_3V)\ \overline{\theta} \tag{5.6}$$

, where g_1 and g_2 are known constants.

In this paper, we compute by using coefficient N and in this case, from the equation (5.6) a_{32} is given by the following:

$$a_{32}=1.3356N(\omega+k_3V)\overline{\theta}. \tag{5.7}$$

We used the values of N shown in Table 5.

We will explain here the concrete computation method.

In the first place, we solve the equation (3.8) by putting $a_{32}=0$ and obtain the value of $\overline{\eta}=\eta_a/\zeta_a$, $\overline{\varphi}=\varphi_a/k_0\zeta_a$, $\overline{\theta}=\theta_a/k_0\zeta_a$, ε_η, $\varepsilon_\varphi$and ε_θ.

Using this computed $\overline{\theta}$ and the equation (5.7), we can get a_{32}, which is used in solving again the equation (3.8).

In this way, computing the equation (3.8) by the iterative method, we finish computing when the error of convergence of θ_a and others settles within 0.1 percents.

The computed results of $\bar{\eta}$, $\bar{\varphi}$ and $\bar{\theta}$ according to the O. S. M. are shown in Figs. 8, 9 and 10.

The response curve of the sway amplitude in Fig. 8 has a hollow near the frequency of the roll resonance. This phenomenon can also be seen for the sway amplitude in beam seas[5]. Such phenomena are due to the coupling of the roll into sway in the roll resonance condition. We will call these phenomena **Coupled Resonance.** This will be discussed in detail in the appendix.

The response curve of the yaw ampiltude in Fig. 9 also has a small hump near the roll resonance condition for the same reason as the sway.

In Fig. 10, the roll amplitudes in the resonance condition become larger with the increase of ship speed. For $M_{\theta e}$, there are few differences between the case of $F_n=0.1$ and the case of $F_n=0.2$, and it can be inferred that the effect of the ship speed upon the roll amplitude in Fig. 10 is due to coupling of sway and yaw into roll.

In the next place, theoretical results $\bar{\eta}$ and $\bar{\theta}$ computed by the new strip theory show good agreement with those by the O. S. M.. There's little difference only for the yaw. This can be seen from the curves of a solid line and a dotted line in Figs. 15~18.

5.2. Comparison between computations and experimental results

Comparisons between Computations and experimental results for the amplitude of motion are shown in Figs. 11~22.

For the sway amplitude in Figs. 11~14, experimental results and computations show satisfactory agreement.

For the yaw amplitude in Figs. 15~18, experimental values are considerably scattered for $\lambda_0/L>1.3$. But it can be generally said that the agreement between the computed and experimental results is satisfactory.

In the comparison of the roll amplitude in Figs. 19~22, the computed values are larger than the experimental ones by 10~20 percents in the resonance conditions.

6. Concluding Remarks

In order to derive the rational method of prediction for the sway, yaw and roll motions in oblique waves, we made such investigations as already discussed in this paper.

We have derived the coupled equations of the sway, yaw and roll motions not only by the O. S. M. but also by Takagi's new strip method.

In the next place, we have got the roll damping moments including the viscous effect and the effect of the ship speed from the free rolling experiments in the still water. And we have let a full ship model self-propel in three nodal waves and measured amplitudes of the sway, yaw and roll motions.

Subsequently, using coefficient N obtained from experiments and equations of motion based on the O. S. M., we have computed amplitudes of the sway, yaw and roll motions in three nodal waves according to the iterative method, and the computation has been also carried out by the new strip method.

Finally, we have compared computed results with experimerntal results.

These investigations may be reduced to the following conclusions.

1) The derivatives of the radiation forces given by the new strip theory show agreement with those by the S. T. F. method excepting end effect.

Difference in them between the former and the O. S. M. appears only for the yaw. This circumstance resembles the one for the longitudinal motions.

2) Difference in the wave exciting force between the new strip method and the O. S. M. also exists only for the yaw.

3) The computed values of the sway and roll amplitudes of the full ship model in three nodal waves differ very little between the new strip method and the O. S. M.. A few differences appear only for the yaw.

4) The agreement between computed and experimental amplitudes of sway and yaw is satisfactory.

5) The amplitude curves of the sway and yaw have a hollow and hump near the roll resonance condition. This is due to the coupling of roll into sway and yaw.

6) The computed values of roll amplitude are larger in the resonance condition than the experimental ones by about 10～20 percents.

Investigations to proceed further would be listed as follows:

a) Improving the computation method of wave exciting forces for an advancing ship, in particular, the roll exciting moment.

b) Measuring radiation derivatives by the forced oscillation method and checking up the equations of motions in this paper.

c) Developing a theoretical equation or an empirical formula to predict correctly the roll damping moment including viscous effect and the effect of advance speed.

Acknowledgments

The author wishes to express his deepest appreciation to Mr. M. Kurihara who carried out numerical computation and he is also gratefall to Mr. H. Arakawa, Mr. T. Kita, Mr. A. Tashiro and other members of the laboratory who cooperated in the model experiments.

It is mentioned that we used in numerical computation FACOM 230-60 of the Computer Center of Kyushu University.

References

1) Eda, H. and Lincoln Crame, C., Steering Characteristics of Ships in Calm Water and Waves, S. N. A. M. E., Vol. 73, 1965.
2) Takezawa, S., Fukuhara, M. and Yamashita, S., On the properties of the Transient Water Waves in Ship Model Basins, J. S. N. A. of Japan, Vol. 124, Dec., 1968.
3) Kurihara, M., Tasai, F. and Suhara, T., On the Experimental Tank for Sea Disasters, J. S. N. A. of West Japan, No. 32, July, 1966.
4) Awaya, Y., Generation of Higher Nodal Waves in Long Basin, Bull. Res. Inst. Appl. Mech., No. 17, 1961.
5) Tasai, F., Ship Motions in Beam Seas, Rep. Res. Inst. Appl. Mech., Vol. XIII. No. 45, 1965.
6) Tasai, F., On the Swaying, Yawing and Rolling Motions of Ships in Oblique Waves, Rep. Res. Inst. Appl. Mech., Vol. XIV. No. 47, 1966.
7) Tasai, F., Improvements in the Theory of Ship Motions in Longitudinal Waves, Appendix II of the Seakeeping Committee, 12th I. T. T. C., 1969.
8) Tasai, F. and Takagi, M., Theory and Calculation of Ship Responses in Regular Waves, Symposium on the Seakeeping Quality, S. N. A. of Japan, July, 1969.
9) Salvesen, N., Tuck, E. O. and Faltinsen, O., Ship Motions and Sea Loads, S. N. A. M. E., Vol. 78, 1970.
10) Tasai, F., On the Equation of Rolling Motion of a Ship, Bull. Res. Inst. Appl. Mech., No. 25, 1965.
11) Tasai, F., Kurihara, M., Arakawa, H., Kawasumi, K. and Kita, T., A Study on the Seakeeping Qualities of Full Ships, J. S. N. A. of West Japan, No. 37, Feb. 1969.
12) Watanabe, Y., Inoue, S. and Murahashi, T., The Modification of Rolling Resistance for Full Ships, J. S. N. A. of West Japan, No. 27, March, 1964.
13) Tasai, F., Kaname, M. and Arakawa, H., Equipment for Measuring Six Motions of Ship Models, Rep. Res. Inst. Appl. Mech., Vol. XIII. No. 45, 1965.
14) Watanabe, Y., On the Motion of the Centre of Gravity of Ships and Effective Wave Slope, J. S. N. A. of Japan, Vol. 49, 1932.
15) Takaki, M., Arakawa, H. and Tasai, F., On the Oscillations of a Semi-Submersible Catamaran Hull at Ballast Condition, J. S. N. A. of West Japan, No. 42, May, 1971. (to be published)
16) Ueno, K., Theory of Free Rolling of Ships, Memoirs of the Faculty of Engineering, Kyushu Imperial University, Vol . 9, 1942.

(Received March 31, 1971)

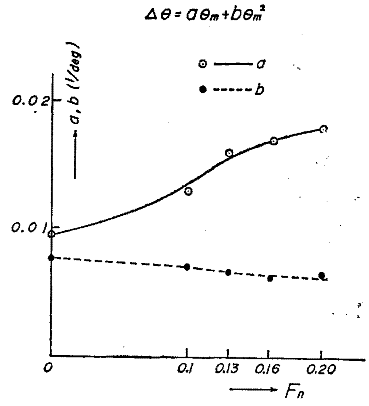

Fig. 5 Coefficients of the cuve of extinction

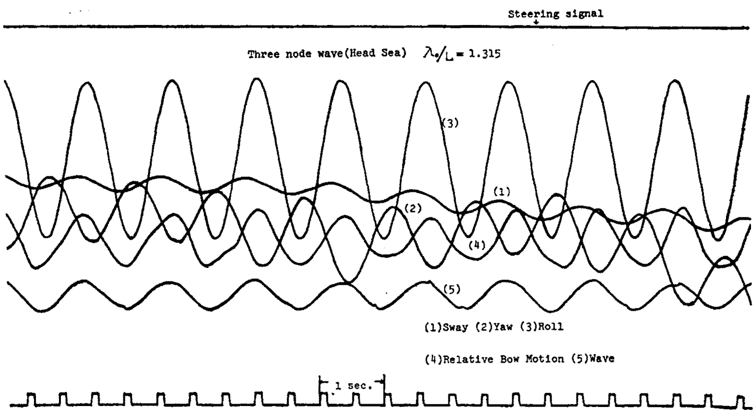

Fig. 6 An illustration of records of ship motions and wave; $\lambda_0/L=1.315$ (wave was recorded on the line of trough and crest)

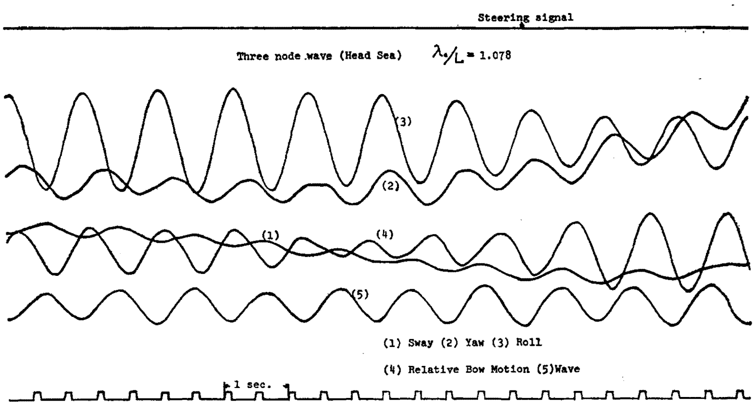

Fig. 7 An illustration of records of ship motions and wave; $\lambda_0/L=1.078$

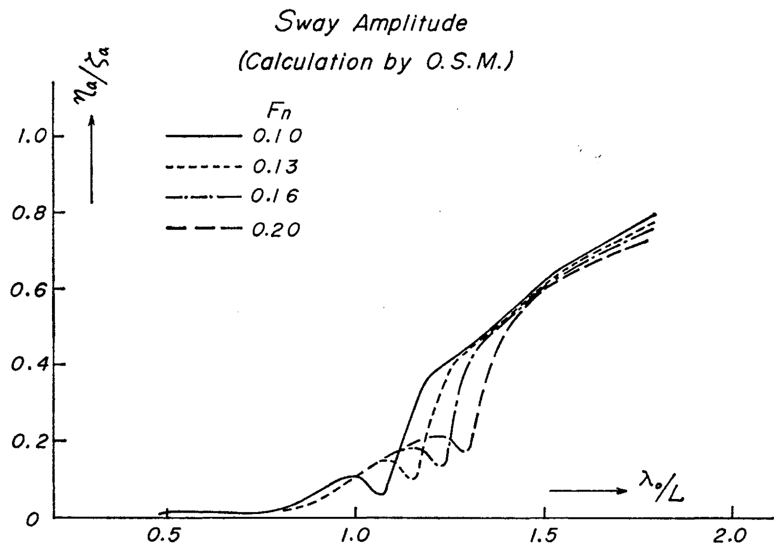

Fig. 8 Calculated frequency characteristics of sway amplitude

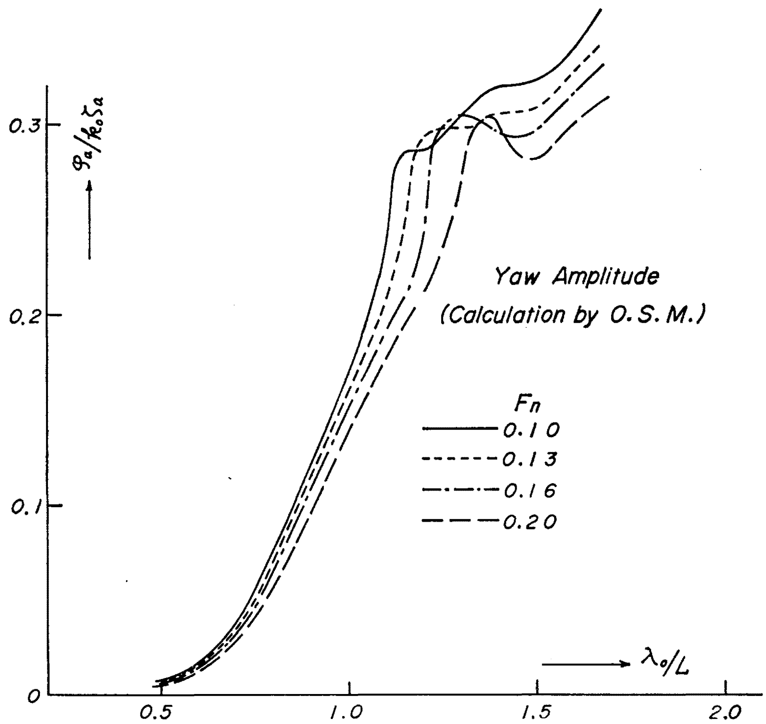

Fig. 9 Calculated frequency characteristics of yaw amplitude

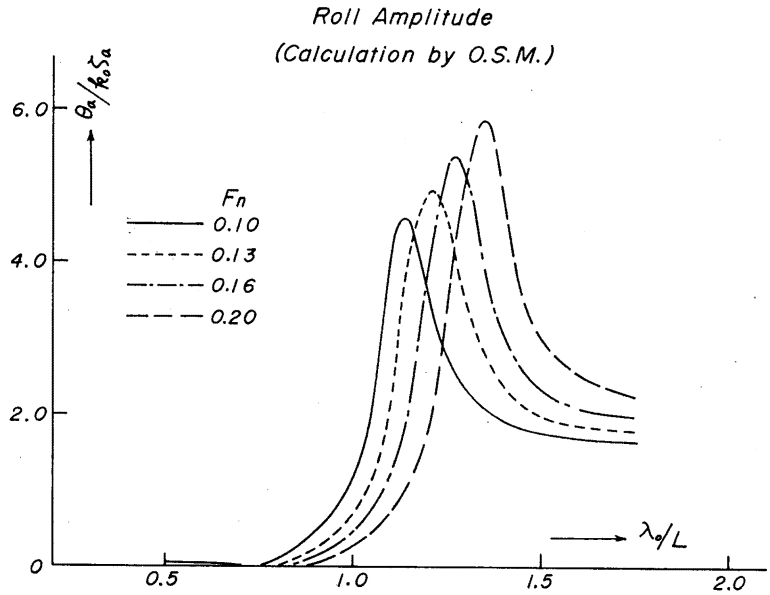

Fig. 10 Calculated frequency characteristics of roll amplitude

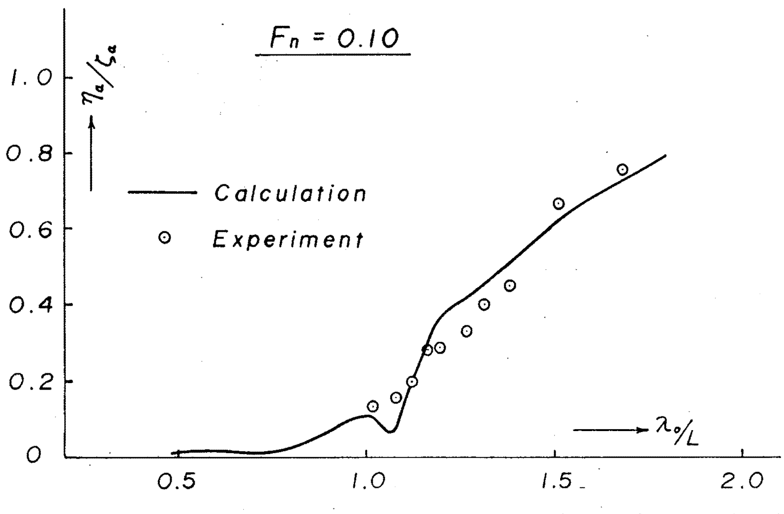

Fig. 11 Comparison of calculated and measured amplitude of sway; $F_n=0.10$

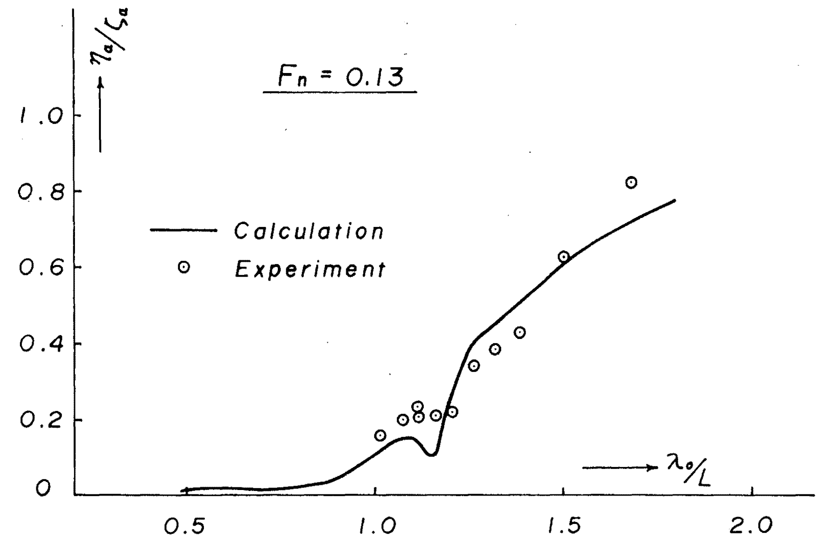

Fig. 12 Comparison of calculated and measured amplitude of sway; F_n=0.13

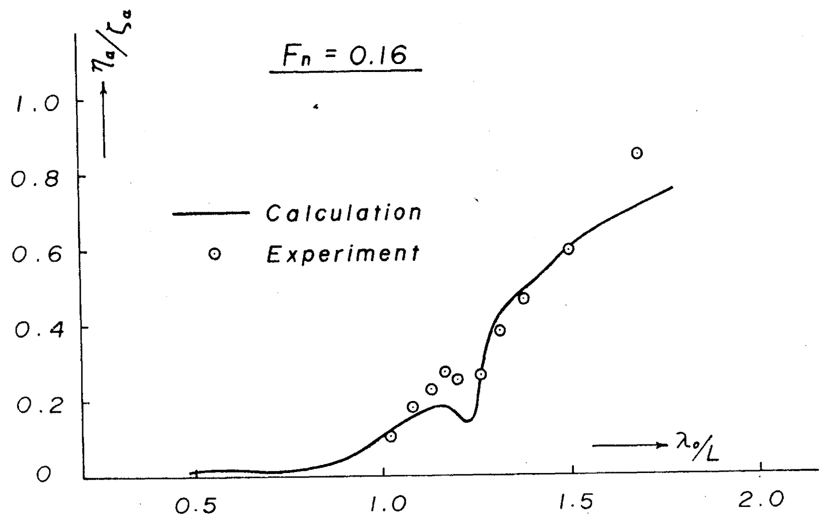

Fig. 13 Comparison of calculated and measured amplitude of sway; F_n=0.16

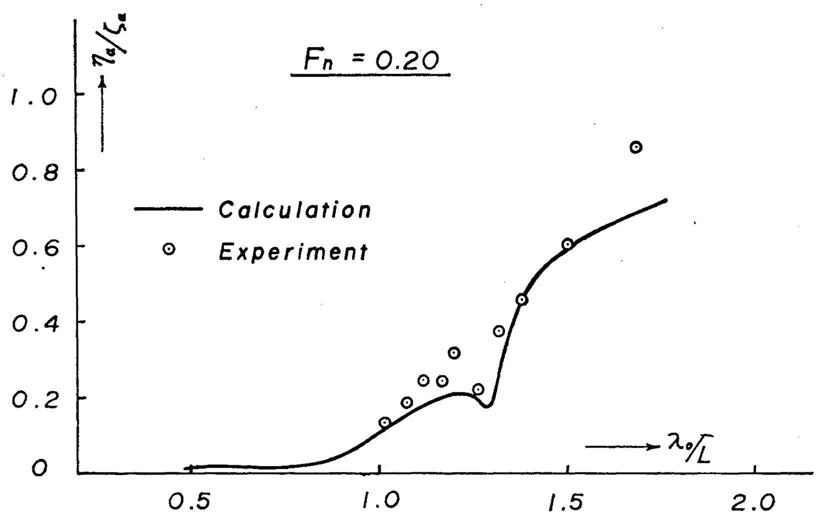

Fig. 14 Comparison of calculated and measured amplitude of sway; F_n=0.20

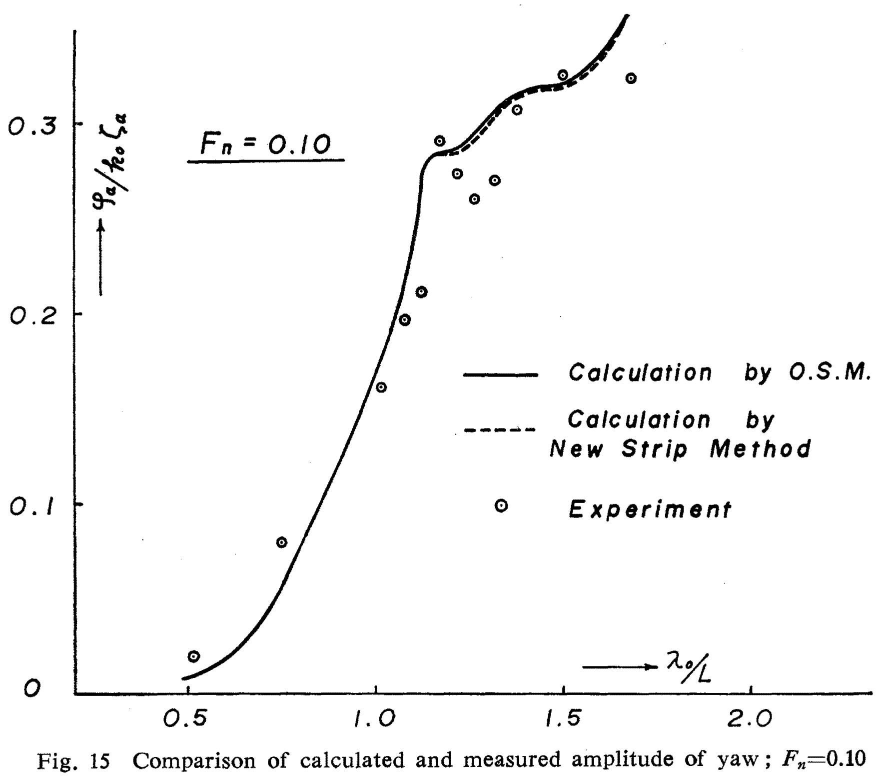

Fig. 15 Comparison of calculated and measured amplitude of yaw; F_n=0.10

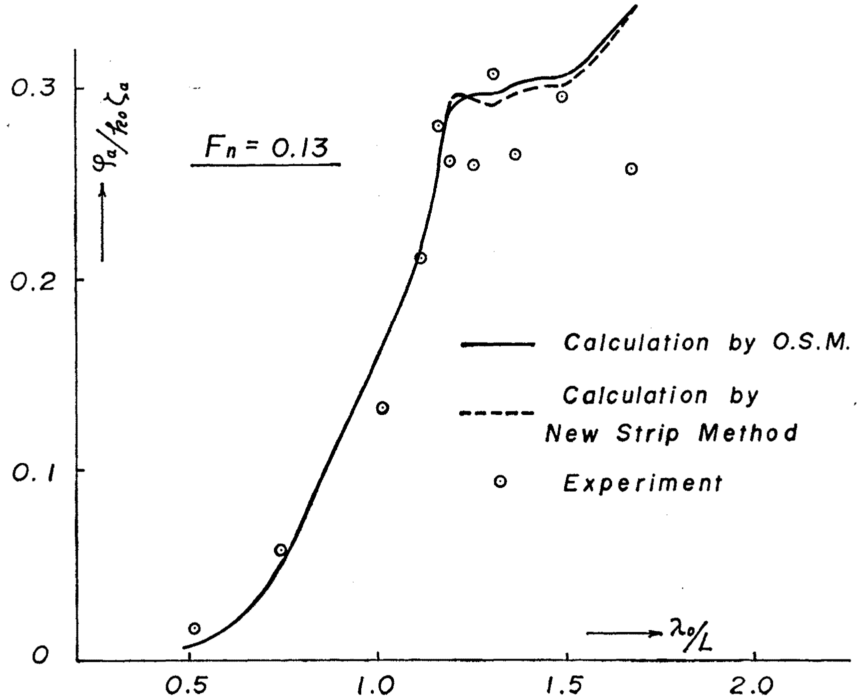

Fig. 16 Comparison of calculated and measured amplitude of yaw; F_n=0.13

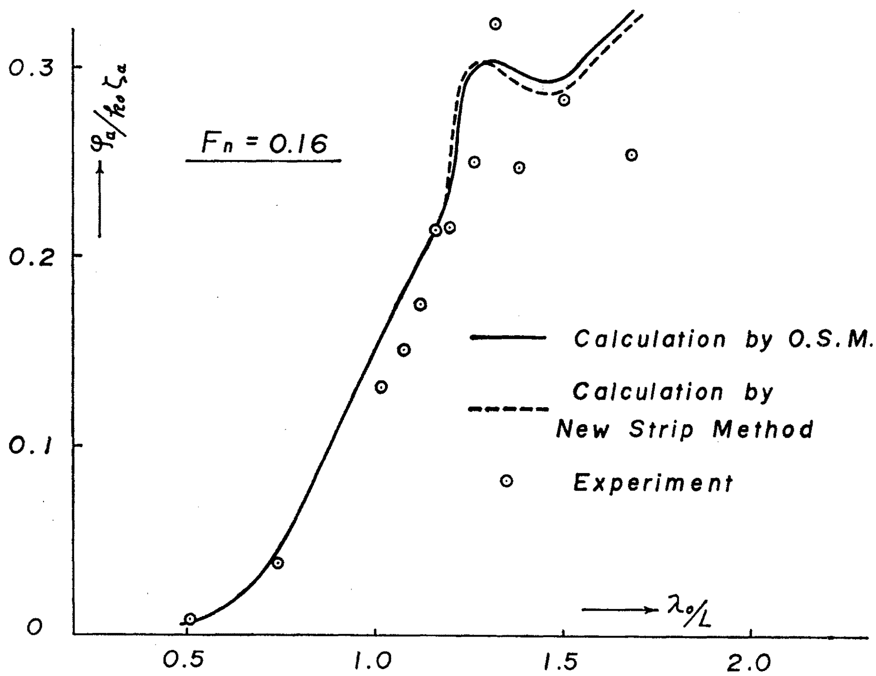

Fig. 17 Comparison of calculated and measured amplitude of yaw; F_n=0.16

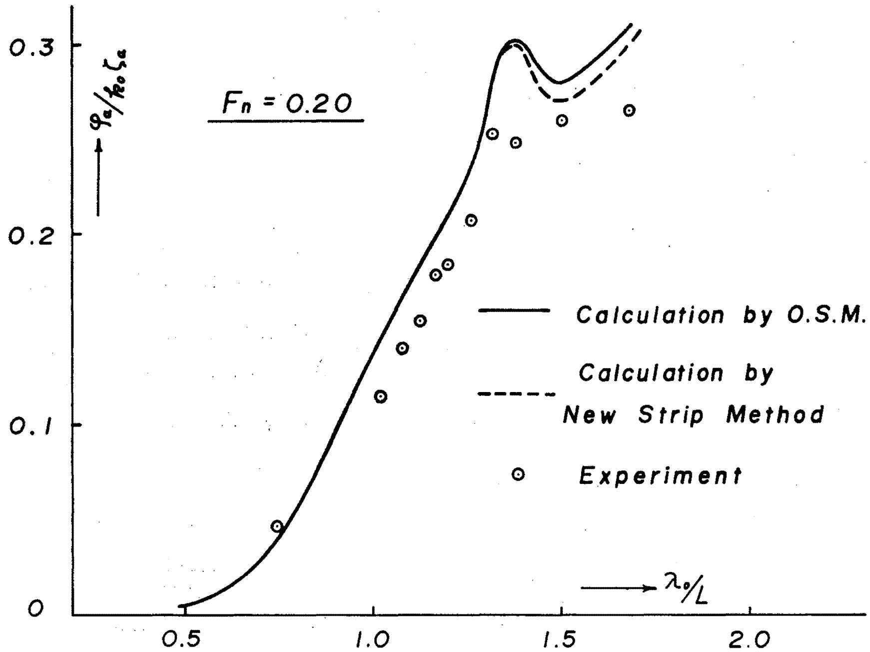

Fig. 18 Comparison of calculated and measured amplitude of yaw; F_n=0.20

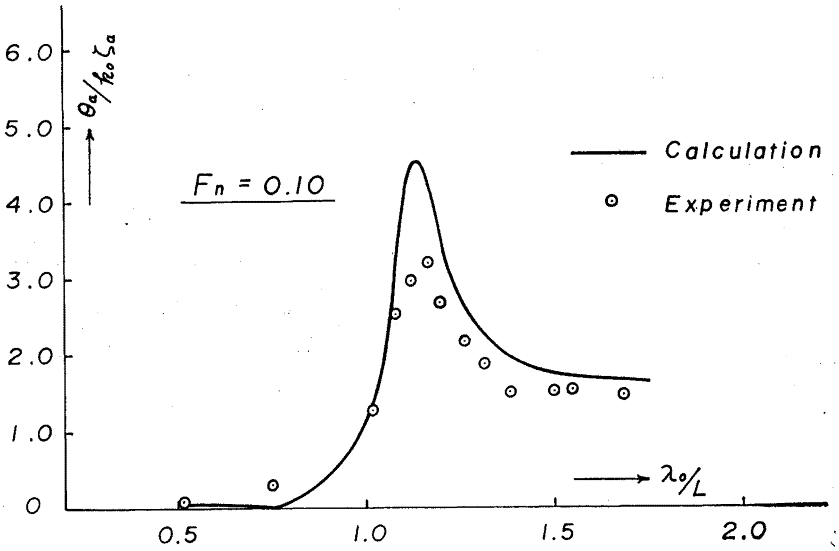

Fig. 19 Comparison of calculated and measured amplitude of roll; F_n=0.10

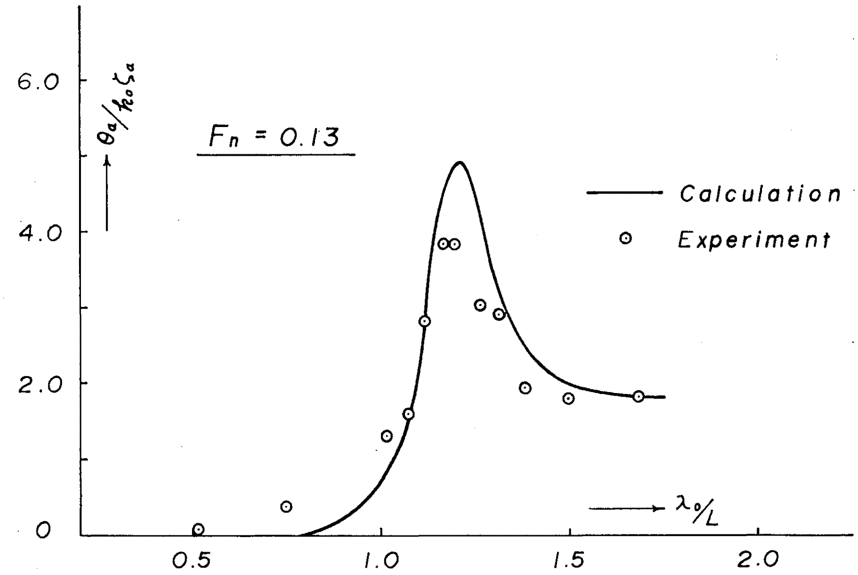

Fig. 20 Comparison of calculated and measured amplitude of roll; F_n=0.13

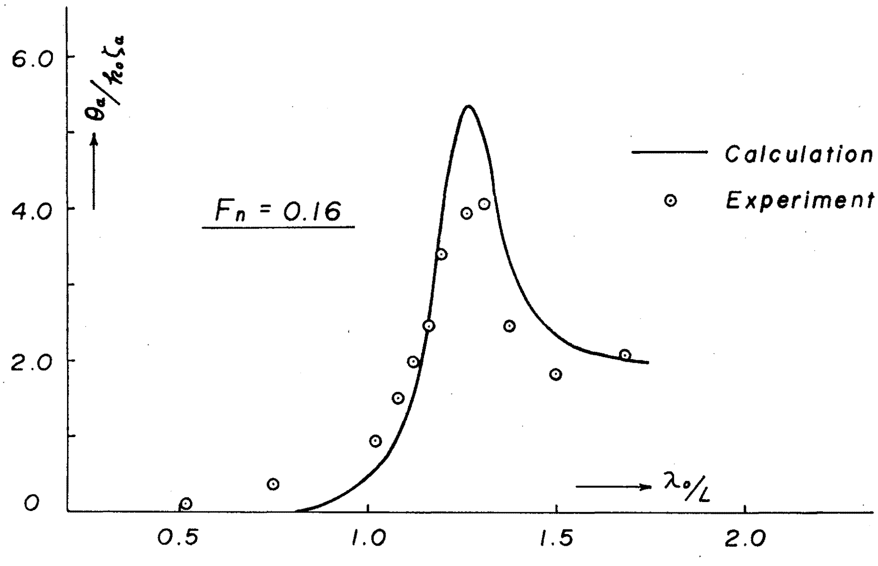

Fig. 21 Comparison of calculated and measured amplitude of roll; F_n=0.16

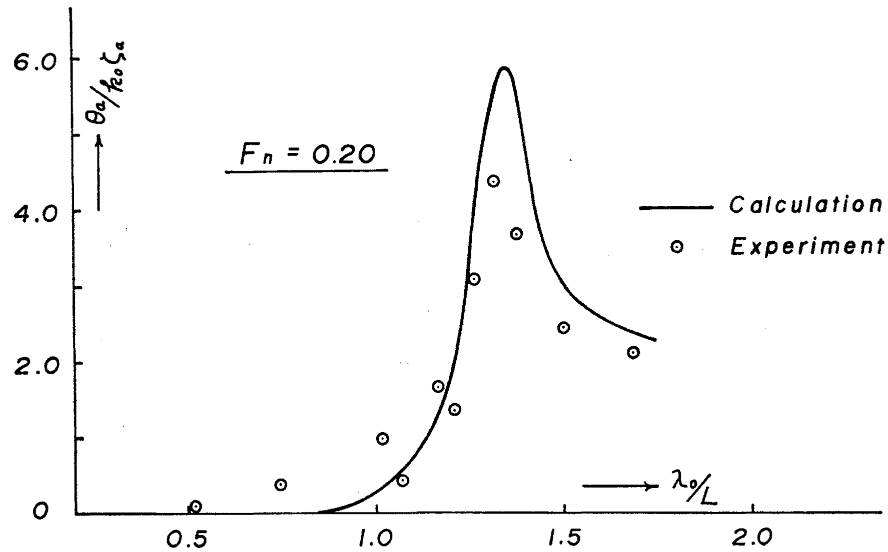

Fig. 22 Comparison of calculated and measured amplitude of roll; F_n=0.20

Appendix

On the Coupled Resonance

In the response curve of the sway amplitude, there appears a hollow near the roll resonance condition, as shown in Fig. 8. Although there is a coupling effect of yaw upon the sway, this phenomenon is mainly due to the coupling of roll into sway in the roll resonance condition.

In the swaying motion of a system with one degree of freedom without the coupling of roll and yaw doesn't exist the natural period of the sway. Accordingly, even if we omit the damping force in this case, it cannot be happened that the sway amplitude of the forced oscillation in waves becomes infinite.

On the other hand, when the sway motion has been coupled into by the roll motion, there appears the resonance peak of the sway amplitude in the forced oscillation.

We will discuss the coupled oscillation of the sway and roll, excepting the yaw in order to make the discussion short.

The natural period of roll is usually calculated from the equation of roll motion of a system with one degree of freedom.

Neglecting the damping moment for the roll, the equation of free rolling is

$$a_{31}\ddot{\theta}+a_{33}\theta=0. \tag{A1}$$

From (A1), the natural circular frequency ω_θ and natural period T_θ of the roll are given by

$$\omega_\theta^2 = a_{33}/a_{31} \text{ and } T_\theta = 2\pi\sqrt{a_{31}/a_{33}} \ . \tag{A2}$$

Putting $\varphi=0$ in the equation (3.8) and considering $a_{13}=c_{13}=b_{33}=0$, the coupled equations of free oscillation are as follows:

$$\left.\begin{aligned} &a_{11}\ddot{\eta}+a_{12}\dot{\eta} \qquad\quad +c_{11}\ddot{\theta}+c_{12}\dot{\theta}=0 \\ &a_{31}\ddot{\theta}+a_{32}\dot{\theta}+a_{33}\theta+b_{31}\ddot{\eta}+b_{32}\dot{\eta}=0 \end{aligned}\right\} \tag{A3}$$

, where $c_{11}=b_{31}$ and $c_{12}=b_{32}$.

The natural period of the coupled oscillation can be approximately calculated from the following equations, omitting the damping forces,

$$\left.\begin{aligned} &a_{11}\ddot{\eta} \qquad\quad +c_{11}\ddot{\theta}=0 \\ &a_{31}\ddot{\theta}+a_{33}\theta+c_{11}\ddot{\eta}=0. \end{aligned}\right\} \tag{A4}$$

Assuming that both η and θ oscillate harmonically with the circular frequency ω, it results that $a_{33}\theta=-\frac{a_{33}}{\omega^2}\ddot{\theta}$.

And (A4) becomes as

$$\left.\begin{aligned} &a_{11}\ddot{\eta}+c_{11}\ddot{\theta}=0 \\ &c_{11}\ddot{\eta}+a_{30}\ddot{\theta}=0 \end{aligned}\right\} \tag{A5}$$

, where $\quad a_{30}=a_{31}-\frac{a_{33}}{\omega^2}$. (A6)

The natural circular frequency ω_n of the coupled oscillation can be got from the following equation:

$$c_{11}a_{30}-c_{11}^2=0. \tag{A7}$$

Consequently, in the case of the undamped oscillation, the amplitudes of η and θ become both infinite if the frequency of the wave exciting force and that of the free oscillation coincide.

For such a phenomenon of resonance as a motion originally without the natural period comes to have by the coupling effect of another motion, we will call the **Coupled Resonance.**

In both computations and experiments of the investigation in this paper did not appear a large resonance amplitude for the sway, however, it is predicted that if the roll damping moment is very small, a large peak of resonance comes out.

The investigations for the coupled motion of the sway and roll for a two dimensional cylinder have been carried out by Mr. M. Takaki and others[15] who omitted the viscous damping. Their calculation shows that a very large resonance amplitude of sway is generated in the resonance condition of the roll.

It is reasonable that the same phenomenon as the sway should consist in the yaw.

We see no examples that a large coupled resonance peak appears for the sway or yaw in the case of an usual ship.
There would be, however, the need to consider the coupled resonance in the case of a marine structure with the multi-hull.

Now, let us suppose $V=0$. In Table 2 can be presented the following:

$$\left.\begin{array}{l} a_{13}=b_{13}=c_{13}=b_{33}=c_{33}=0,\ c_{21}=b_{21}, \\ c_{22}=b_{12},\ b_{21}=c_{31},\ b_{22}=c_{32},\ b_{31}=c_{11} \text{ and } b_{32}=c_{12}. \end{array}\right\} \tag{A8}$$

Then, the equation of the free oscillation can be written, using (A6) in the form:

$$\left.\begin{array}{l} a_{11}\ddot{\eta}+a_{12}\dot{\eta}+b_{11}\ddot{\varphi}+b_{12}\dot{\varphi}+c_{11}\ddot{\theta}+c_{12}\dot{\theta}=0 \\ b_{11}\ddot{\eta}+b_{12}\dot{\eta}+a'_{21}\ddot{\varphi}+a_{22}\dot{\varphi}+b'_{21}\ddot{\theta}+b_{22}\dot{\theta}=0 \\ c_{11}\ddot{\eta}+c_{12}\dot{\eta}+b_{21}\ddot{\varphi}+b_{22}\dot{\varphi}+a_{30}\ddot{\theta}+a_{32}\dot{\theta}=0 \end{array}\right\} \tag{A9}$$

, where $a'_{21}=a_{21}-\dfrac{a_{23}}{\omega^2}$ and $b'_{21}=b_{21}-\dfrac{c_{23}}{\omega^2}$.

Coefficients of $a_{11}, \ldots\ldots, a_{32}$ in the above equations are generally functions of circular frequency ω, and therefore, it is very hard to compute the coupled natural frequency from (A9).

Omitting items of damping forces, that is, items of $\dot{\eta}$, $\dot{\varphi}$ and $\dot{\theta}$ in (A9), we can get graphically the coupled natural frequency of the undamped oscillation by the following:

$$\Delta=\begin{bmatrix} a_{11} & b_{11} & c_{11} \\ b_{11} & a'_{21} & b'_{21} \\ c_{11} & b_{21} & a_{30} \end{bmatrix}=0. \tag{A 10}$$

Hereafter, we will discuss the coupled natural frequency of the sway and roll.

The coupled free oscillation of the sway and roll has been studied in detail by Dr. Ueno[16].

In the first place, he derived the following coupled equations of the sway and roll.

$$\left.\begin{array}{l} (I+I_1h_1)\ddot{\theta}+I_{10}h_1\dot{\theta}+WGM\theta-(M_1\ddot{\eta}+M_{10}\dot{\eta})h_2=0 \\ (M+M_1)\ddot{\eta}+M_{10}\dot{\eta}-(I_1\ddot{\theta}+I_{10}\dot{\theta})=0. \end{array}\right\} \tag{A 11}$$

Solving the above equations of motions, he showed that the roll motion θ is approximately expressed by the following form of the damped oscillation:

$$\theta=\theta_0\sec\sigma e^{-\alpha t}\cos(\omega_n t-\sigma) \tag{A 12}$$

and that the sway motion η is composed of one aperiodic damped horizontal translation and one damped horizontal oscillation, as shown in the following:

$$\eta \doteqdot \theta_0 R_2 \sec\sigma \left[e^{-\gamma t} \frac{\mu}{\gamma} \sin\varepsilon + e^{-\alpha t} \cos(\omega_n t - \sigma - \varepsilon) \right] \tag{A 13}$$

According to him, the center of gravity of the ship translates transversely toward the opposite direction to the side to which a ship is initially forced to list by external moment, oscillating horizontally.

The oscillation gradually damps with the horizontal shift of the center of gravity.

In the next place, he calculated the roll motion of the ship, whose horizontal motion of the center of the gravity was strictly restrained.

Furthermore, using the model ship (Lpp=189.2 cm, $H_0=B/2d=1.08$, with bilge keel), he carried out two kinds of experiments; one is the coupled free oscillation and the other is the free rolling of the ship model whose horizontal translation is strictly restrained.

He obtained the following results.

1) The coupling effect of the horizontal motion on the damping coefficient of the roll decreased with the increase of the value of θ_a: about 7 percents at $\theta_a=0$, about 4 percents at $\theta_a=35$ degrees.

2) The coupling effect of the horizontal motion on the natural rolling period showed as small a value as about 2 percents irrespective of θ_a.

From the above he concluded that the influences of the horizontal motion upon the damping power and the period of free rolling are small enough to be neglected.

Now, in the case of zero speed, from the Table 2 we obtain

$$a_{11} = m_0(1+\overline{K}_\eta),$$

$$a_{30} = (J_x + I_{x0}) - \frac{W \cdot GM}{\omega^2},$$

$$c_{11} = \int_L m'(l_\eta - \overline{O_1G})\, dx_b.$$

Using the above, the equation (A7) is transformed into the following equation:

$$(J_x + I_{x0}) - \frac{W \cdot GM}{\omega^2} = \frac{\left[\int_L m'(l_\eta - \overline{O_1G})\, dx_b \right]^2}{m_0(1+\overline{K}_\eta)} \tag{A 14}$$

Putting
$$(J_x + I_{x0}) - \frac{\left[\int_L m'(l_\eta - \overline{O_1G})\, dx_b \right]^2}{m_0(1+\overline{K}_\eta)} = G(\omega) \tag{A 15}$$

, we can obtain the natural circular frequency by the graphical method as shown in Fig. A1.

In the case of an usual ship, because the value of K_η would be positive, ω is always larger than ω_θ obtained from $a_{30}=0$.

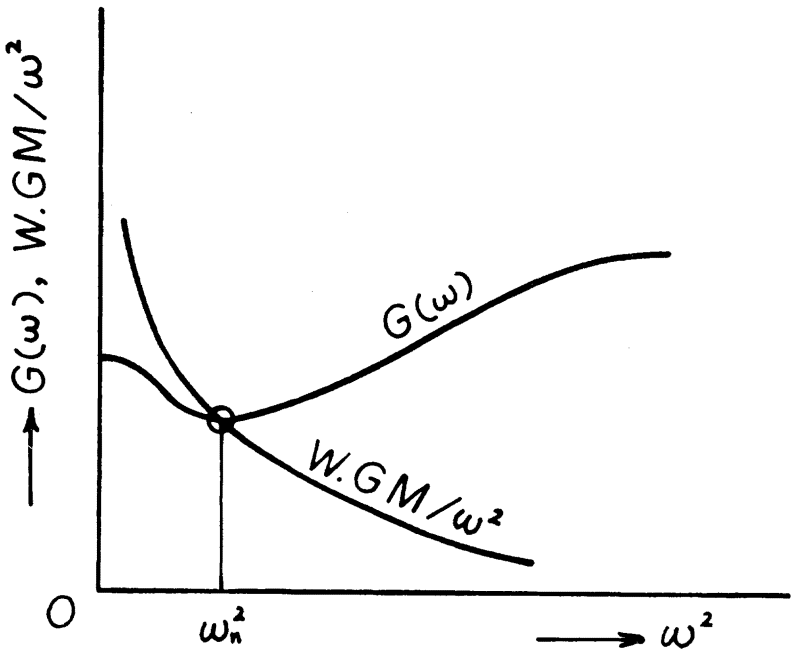

Fig. A1

Herein, putting

$$\left[\int_L m'(l_\eta - \overline{O_1G})\, dx_b\right]^2 / m_0(1+\overline{K}_\eta) = \delta \qquad \text{(A 16)}$$

, the difference between ω_0 and ω_n becomes larger as δ increases.

For example, we will compute the approximate value of δ for a two dimensional body, whose section is the Lewis form ($H_0=2.0$ and $\sigma=\dfrac{S_w}{2bT}=0.9$).

From the appendix of the paper[8] we obtain $K_s=m'/\rho S_w=0.7$ and $L_{SR}/T=-0.8$ in the small circular frequency. And therefore, we have $m'=1.26\ \rho bT$, $l_\eta=-0.8T$ and $m_0=1.8\ \rho bTL$.

Assuming the $\overline{O_1G}$ is much smaller than l_η and neglecting the value of $\overline{O_1G}$ we obtain

$$\delta = 0.332\ \rho bT^3L.$$

Putting $\delta = m_0(K2b)^2$

, we get $K = 0.107$.

Accordingly, in this case, it results that the radius of gyration is $0.214b$ less than the one computed from the equation of roll of a system with one degree of freedom.